CORNELL AERONAUTICAL LABORATORY, INC.
BUFFALO, NEW YORK

FLIGHT RESEARCH DEPARTMENT

FULL-SCALE DIVISION MEMORANDUM (FDM) NUMBER 377

THEORY AND ANALYSIS OF A HIGHLY ELASTIC LAUNCH VEHICLE

April 1966

Prepared by: Josef L. Francis

Approved by: E G Rynaski

E M Ball

PRECEDING PAGE BLANK NOT FILMED.

TABLE OF CONTENTS

LIST OF TABLES AND ILLUSTRATIONS

LIST OF SYMBOLS

A	cross sectional reference area, m^2
a_z	acceleration, m/sec^2
BM	bending moment, m-kg
C_{z_α}	variation of normal force coefficient with angle of attack, 1/rad
D_R	rigid body characteristic equation
D_{B_2}	first and second bending mode characteristic equation
D_{B_4}	first, second, third, fourth bending mode characteristic equation
$D(s)$	characteristic polynomial of open-loop plant
$\bar{D}(s)$	$\bar{D}(s) = D(-s)$
$E_{(x)}$	modulus of elasticity at any station x, kg/m^2
F	total thrust of the vehicle, kg
g	gravitational acceleration, m/sec^2
I_e	engine moment of inertia, $kg\text{-}m\text{-}sec^2$
I_y	moment of inertia of the pitch plane, $kg\text{-}sec^2\text{-}m$
$I_{(x)}$	area moment of inertia of the cross section, m^4
$K_i(t)$	time dependent coefficient
l	length of beam, m
m	total mass of the vehicle, $kg\text{-}sec^2/m$
m_e	engine mass, $kg\text{-}sec^2/m$
$\mathcal{M}_i$	generalized mass, $kg\text{-}sec^2/m$
x_i	body station i, m
$Y_{i(x_i)}$	normalized displacement at station x_i, unitless
$Y'_{i(x_i)}$	normalized slope at station x_i, 1/m
$\bar{Z}$	direction normal to reference ($\bar{X}$), m
α	angle of attack, rad

β_c	control deflection angle command, rad
β_L	control deflection angle, rad
$\Delta(s)$	characteristic polynomial of the optimal system
ζ_i	damping ratio of the i^{th} bending mode, unitless
η_i	generalized displacement of the i^{th} mode, m
ϕ	attitude angle, rad
x	state variable
ω_i	bending frequency of the i^{th} mode, rad/sec
$M_{(x)}$	moment distribution along the length of the beam, kg-m/m
$m_{(x)}$	mass distribution along the length of the bean, kg-sec^2/ m^2
$P_{(x)}$	load distribution along the length of the beam
$\bar{q}$	dynamic pressure, kg/m^2
$Q_i(t)$	generalized force for the i^{th} mode, kg
q_i	weighting factors of the performance index
R'	total thrust of control engines (= 1/2 F), kg
r	weighting factor of theperformance index
s	Laplace transform variable
$S_{(x)}$	shear distribution along the length of the beam
t	time, sec
u	optimal feedback control law
V	velocity, m/sec or the performance index $\left(= \frac{1}{2} \int_0^{\infty} (q_1 \phi^2 + q_2 \eta_2^2 + q_3 \eta_1^2 + r \beta_c^2) dt\right)$
$\dot{v}_a$	axial component of acceleration, m/sec^2
$\dot{v}_T$	tangential component of acceleration, m/sec^2
$w(x,t)$	force distribution over the length of the vehicle for all forces acting upon the vehicle, kg/m
X	drag force, kg

Matrices

F	matrix of constants that define the interactions among the state variables
G	matrix of constants defining the effect of a control on the state rates
H	matrix transformation on x that defines the output, $y = Hx$
K	feedback gain matrix
Q	matrix of weighting factors of the performance index
R	matrix of constants weighting the control in the performance index

Subscripts

CG	center of gravity
CP	center of pressure
e	engine
i	i^{th} bending mode
n	station index
PG	position gyro
R	rigid body
RG	rate gyro
x_β	gimbal point body station
x_ϕ	sensor body station

1.0 INTRODUCTION

The equations presented in this FDM were obtained for use in a program designed to investigate the application of optimal control techniques to the control of a highly elastic launch vehicle. The work was performed for the George C. Marshall Space Flight Center under Contract NAS8-20067. The primary aim of the program is the analysis and synthesis of an optimal control system for controlling the bending modes of an elastic launch vehicle.

The equations of motion for the rigid body, the bending modes, and engine-actuator dynamics have been simplified to reduce their complexity without significantly altering the vehicle characteristics in the frequency range of interest. For the vehicle used in this investigation, there is little coupling among the roll, pitch, and yaw degrees of freedom because of the structural and inertial symmetry and because of the relatively small aerodynamic surfaces. Therefore, the pitch and yaw motions can be investigated separately. Also due to symmetry, the equations of motion in the yaw plane are the same as the equations in the pitch plane.

In point-time investigations, the forward velocity is assumed to be constant at the velocity of the nominal trajectory. Hence, there are two degrees of freedom in the pitch plane: rotation and normal translation. Figures 1 and 2 show the pitch plane with each parameter shown in its positive sense.

The purpose of Sections 2 and 3 is to provide insight to the terms in the equations, to the simplifications made, and to the vehicle's modes of motion. Small perturbation equations are used for the control studies. Hence, only small deviations of pitch angle (ϕ) and angle of attack (α) in the plane of motion are allowed about the nominal flight trajectory with the stability derivatives and dynamic pressure assumed constant.

In order to describe the motions of the flexible vehicle, a modal approach is used. The shape of the deflected vehicle is obtained by the summation of selected mode shapes. Three assumptions were made in determining the mode shapes:

1. the liquids in the tanks were considered rigid in the sectional mass distribution,
2. the engines were rigidly attached with the mass of the engines lumped at the engine center of gravity body station, and
3. the mode slope is constant aft of the gimbal station.

As shown in Table IV, the mode shapes are normalized to a value of unity at station 0 and are computed so that there is no elastic or inertial coupling. However, the flexible modes are aerodynamically coupled and coupled through the control system.

Finally, Section 4 presents an example of an optimal control technique as applied to the control of a highly elastic launch vehicle. In this example, only the first and second bending modes are considered. A performance index was selected and the closed-loop poles were obtained. Finally, the feedback control law was computed.

2.0 SYSTEM EQUATIONS OF MOTION

2.1 PITCH ACCELERATION EQUATIONS

The pitch acceleration equation about the center of gravity can be derived from Figures 1 and 2. If the torques acting on the vehicle are summed and then divided by the pitch plane moment of inertia, the following equation is obtained.

$$\ddot{\phi} + \frac{\bar{q} A C_{z_\alpha}(x_{CG}-x_{CP})}{I_y}\alpha + \sum_i \left[\frac{F}{I_y} Y_{i(x_\beta)} - \frac{F(x_{CG}-x_\beta)}{I_y} Y'_{i(x_\beta)} - 4\left(\frac{F-X}{m}\right)\frac{m_e(x_\beta-x_e)}{I_y} Y'_{i(x_\beta)}\right]\eta_i + 4\left[\frac{(x_{CG}-x_\beta)m_e(x_\beta-x_e)+I_e}{I_y}\right]\ddot{\beta}_L$$
$$+ \left[4\,\frac{F-X}{m}\,\frac{m_e(x_\beta-x_e)}{I_y} + \frac{R'(x_{CG}-x_\beta)}{I_y}\right]\beta_L = 0 \tag{1}$$

The above equation assumes that small angle approximations are valid (i.e., $\sin\beta_L \approx \beta_L$, $\sin\alpha \approx \alpha$, etc.). Since there are no large aerodynamic lifting surfaces, the aerodynamic damping term $(D/I_y)\dot{\phi}$ is assumed negligible and omitted.

The aerodynamic and inertial torques can be easily seen in Figure 1. Due to bending, the thrust (F) does not act along the x body axis. This change in the direction of the thrust introduces additional torques which are shown in Figure 2. From Figure 2, we can sketch the following:

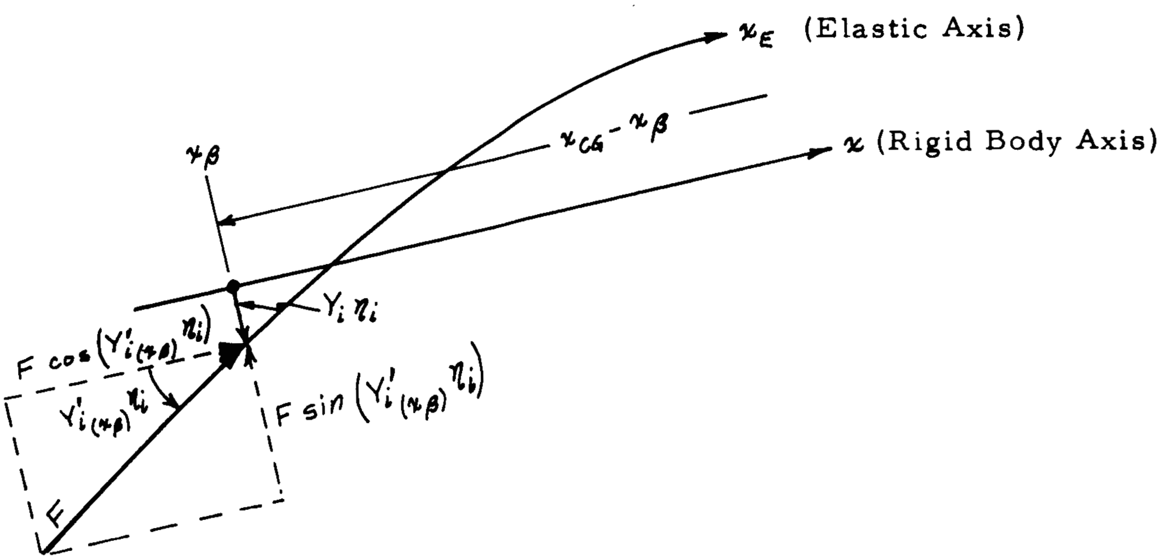

Sketch A

Sketch A shows the thrust in component form with the appropriate moment arms. Assuming small angle approximations (i.e., $\sin Y'_{i(x_\beta)}\eta_i = Y'_{i(x_\beta)}\eta_i$ and $\cos Y'_{i(x_\beta)}\eta_i = 1$), the following torques are obtained:

$$-\sum_i F Y'_{i(x_\beta)}\eta_i + \sum_i F(x_{CG} - x_\beta) Y'_{i(x_\beta)}\eta_i$$

When the control engines are being deflected at an angular acceleration, $\ddot{\beta}_L$, about the gimbal pivots, there results an inertial torque ($4I_e\ddot{\beta}_L$).

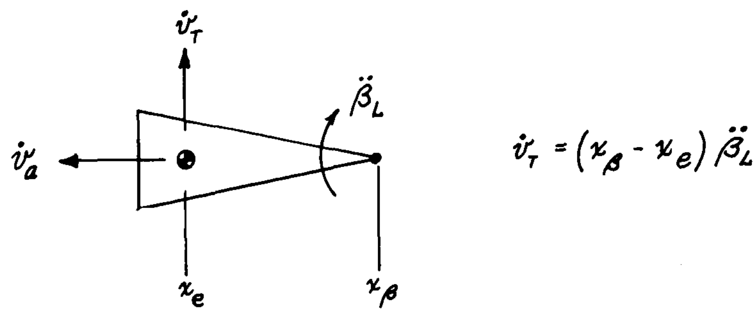

Sketch B

This inertial torque can be transferred to the center of gravity of the vehicle.

In Sketch B, the axial and tangential components of acceleration caused by gimballing the control engines are shown. The component of force due to the axial component of acceleration is negligible compared to the total thrust (F) and therefore it was omitted. The component of force due to the tangential acceleration is

$$4m_e(x_\beta - x_e)\ddot{\beta}_L$$

The pitching moment about the center of gravity of the vehicle due to this inertial reaction force is

$$4(x_{CG} - x_\beta)m_e(x_\beta - x_e)\ddot{\beta}_L$$

The factor 4 is needed for the above two inertial torques because four engines are gimballed together.

In addition to the above torques, a control torque $R'(x_{CG} - x_\beta)\beta_L$ is generated when $\beta_L \neq 0$ which is easily derived from Figure 1. In addition to the thrust vectoring torque, a small torque is generated by the shift in the engine mass. This can be derived from Figure 2 or Sketch C.

Assuming that the axial acceleration $\left(\frac{F-X}{m}\right)$ of the launch vehicle is invariant with bending, then the acceleration of the engines is $\left(\frac{F-X}{m}\right)$. The displacement (moment arm) of the engine center of mass is $(x_\beta - x_e)\sin(\beta_L - Y'_{i(x_\beta)}\eta_i)$. Assuming that small angle approximations are valid, the torque due to engine displacement is

$$4\frac{F-X}{m}m_e(x_\beta - x_e)(\beta_L - Y'_{i(x_\beta)}\eta_i)$$

Data for computing the coefficients of Equation 1 are tabulated in Tables I, II, IV.

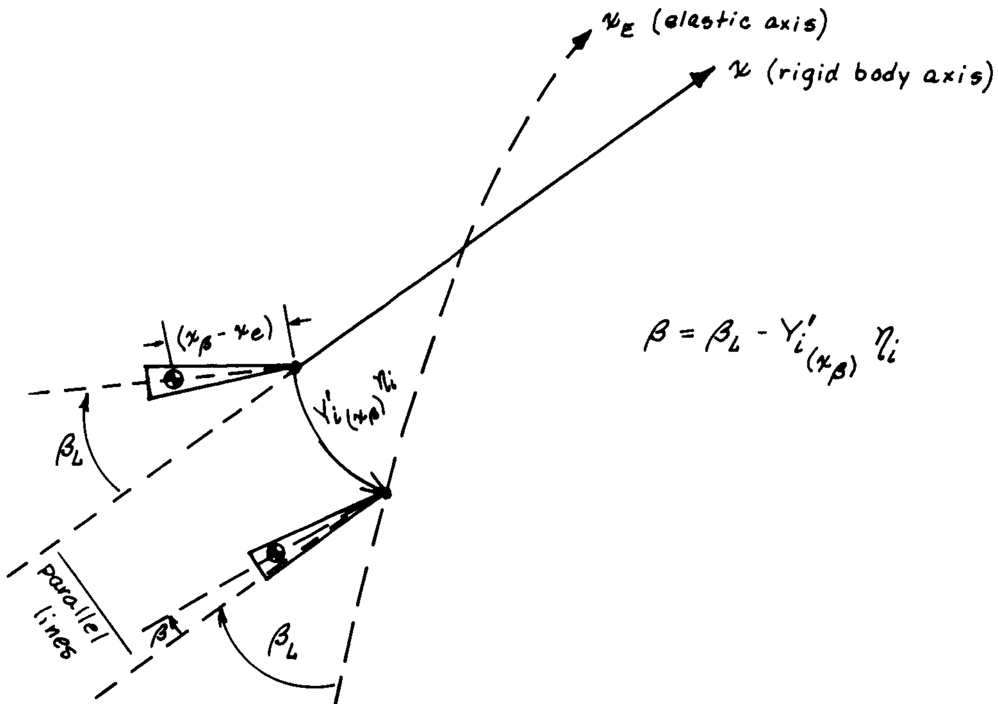

Sketch C

2.2 ACCELERATION EQUATION IN $\bar{Z}$ DIRECTION

The acceleration of the center of gravity in the $\bar{Z}$ direction can be obtained from Figures 1 and 2 by summing the forces in the $\bar{Z}$ direction and dividing by the total mass:

$$\ddot{\bar{Z}} = \frac{F-X}{m}\phi + \frac{\bar{q}AC_{z_\alpha}}{m}\alpha - \frac{F}{m}\sum_i Y'_{i(x_\beta)}\eta_i + \frac{R'}{m}\beta_L - V\dot{\psi} + g\sin\psi \qquad (2)$$

Equation 2 assumes that small angle approximations are valid. The last two terms of Equation 2 account for the difference between the centrifugal and gravitational accelerations. Most trajectories are shaped such that the vehicle flies a gravity turn trajectory (i.e., a zero lift or zero angle of attack trajectory). Therefore,

$$\dot{\psi} = \frac{g\sin\psi}{V}$$

and the last two terms of Equation 2 cancel. If this type of a trajectory is not flown, these two terms should be included.

Since $\bar{Z}$ will introduce an additional variable into the system of equations which cannot be measured directly and used in the synthesis of a control system, it is desirable to eliminate it. This can be done by differentiating, with respect to time, the angular equation shown in Figure 1 and solving for $\ddot{\bar{Z}}$.

$$\ddot{\bar{Z}} = V(\dot{\phi} - \dot{\alpha}) \qquad (3)$$

Velocity is constant for a point-time investigation. If Equation 3 is substituted into Equation 2, the $\ddot{Z}$ equation becomes

$$-\dot{\phi} + \frac{F-X}{mV}\phi + \dot{\alpha} + \frac{\bar{q}AC_{z_\alpha}}{mV}\alpha - \frac{F}{mV}\sum_i Y'_{i(x_\beta)}\eta_i + \frac{R'}{mV}\beta_L = 0 \tag{4}$$

The terms $\left(\frac{F-X}{m}\phi\right)$, $\left(\frac{\bar{q}AC_{z_\alpha}}{m}\alpha\right)$, and $\left(\frac{R'}{m}\beta_L\right)$ are easily derived from Figure 1. The $\dot{\phi}$ and $\dot{\alpha}$ terms were obtained from the $\ddot{Z}$ substitution. Finally, the bending term $\left(-\frac{F}{m}\sum_i Y'_{i(x_\beta)}\eta_i\right)$ is easily obtained from Sketch A in Section 2.1. The data for computing the coefficients of Equation 4 are tabulated in Tables I, II, and IV.

2.3 BENDING EQUATION

A typical launch vehicle can be represented by a nonuniform free-free beam with arbitrary mass and stiffness distribution. The loading on the vehicle can be both static and dynamic, and the bending is assumed to be in the lateral direction only. A free-free beam with arbitrary loading is shown in Figure 3. The differential relationship between the deflection z and the bending moment M is

$$\frac{\partial^2 z}{\partial x^2} = \frac{M(x)}{E(x)I(x)} \tag{5}$$

The load distribution $P(x)$ is equal to

$$P(x) = \frac{\partial}{\partial x}\left[S(x)\right] \tag{6}$$

where $S(x)$ is the shear distribution.

$$S(x) = \frac{\partial}{\partial x}\left[M(x)\right] \tag{7}$$

Hence, Equation 6 can be written as

$$P(x) = \frac{\partial^2}{\partial x^2}\left[M(x)\right] \tag{8}$$

If $M(x)$ of Equation 5 is substituted into Equation 8, the plane elastic motion of the beam is described by the resulting partial differential equation

$$\frac{\partial^2}{\partial x^2}\left[E(x)I(x)\frac{\partial^2 z}{\partial x^2}\right] = P(x) \tag{9}$$

It is now assumed that the mass of the beam and its elastic properties can be considered separately. Therefore, the beam will be considered a massless elastic body with masses attached to it. Also, it is assumed that no external forces or constraints are acting on the beam (free-free). Since the beam is moving in free vibration, the beam will be loaded by inertial forces. Therefore,

$$P(x) = -m(x) \frac{\partial^2 z}{\partial t^2} \tag{10}$$

and Equation 9 becomes

$$m(x) \frac{\partial^2 z}{\partial t^2} + \frac{\partial^2}{\partial x^2} \left(E(x) I(x) \frac{\partial^2 z}{\partial x^2} \right) = 0 \tag{11}$$

where m(x), I(x), and E(x) are functions of x and must always be positive.

The deflection z from the undeflected elastic axis is represented by a Fourier series of normal mode functions:

$$z(x,t) = \sum_i Y_{i(x)} \eta_i (t) \tag{12}$$

where $Y_{i(x)}$ is the normalized displacement at station x_i and $\eta_i(t)$ is the generalized displacement of the i^{th} mode. Values of $Y_{i(x)}$ along the vehicle are tabulated in Table IV for the first four bending modes.

2.3.1 EXTERNAL LOADING

If the vehicle is subjected to external loading, $w(x,t)$, then Equation 11 becomes

$$m(x) \frac{\partial^2 z}{\partial t^2} + \frac{\partial^2}{\partial x^2} \left(E(x) I(x) \frac{\partial^2 z}{\partial x^2} \right) = w(x,t) \tag{13}$$

Now, if Equation 13 is multiplied by $Y_{i(x)}$, it becomes

$$m(x) Y_{i(x)} \frac{\partial^2 z}{\partial t^2} + \frac{\partial^2}{\partial x^2} \left[E(x) I(x) \frac{\partial^2 z}{\partial x^2} \right] Y_{i(x)} = w(x,t) Y_{i(x)} \tag{14}$$

Differentiating Equation 12 with respect to time (t) and x, we get

$$\frac{\partial z}{\partial t} = Y_{i(x)} \dot{\eta}_i$$

and

$$\frac{\partial^2 z}{\partial t^2} = Y_{i(x)} \ddot{\eta}_i \tag{15}$$

$$\frac{\partial z}{\partial x} = \frac{\partial Y_{i(x)}}{\partial x} \eta_i$$

$$\frac{\partial^2 z}{\partial x^2} = \frac{\partial^2 Y_{i(x)}}{\partial x^2} \eta_i \tag{16}$$

Substituting Equations 15 and 16 into Equation 14 gives

$$m(x)\left[Y_{i(x)}\right]^2\ddot{\eta}_i + \frac{\partial^2}{\partial x^2}\left[E(x)I(x)\frac{\partial^2 Y_{i(x)}}{\partial x^2}\right]Y_{i(x)}\,\eta_i = w(x,t)\,Y_{i(x)} \tag{17}$$

Assuming that w(x, t) can be represented in a manner which is similar to Equation 12, then

$$w(x,t) = \sum_i K_i(t)\,m(x)\,Y_{i(x)} \tag{18}$$

where $K_i(t)$ is an unknown function. Integrating $w(x,t)\,Y_{i(x)}$ over the length (ℓ) of the vehicle, we get

$$\int_0^{\ell} w(x,t)\,Y_{i(x)}\,dx = \sum_i K_i(t)\int_0^{\ell} m(x)\,Y_{i(x)}^{\,2}\,dx \tag{19}$$

Hence, $K_i(t)$ is found to be

$$K_i(t) = \frac{\int_0^{\ell} w(x,t)\,Y_{i(x)}\,dx}{\int_0^{\ell} m(x)\,Y_{i(x)}^{\,2}\,dx} \tag{20}$$

In References 1, 2 and 3, the numerator of Equation 20 is called the generalized force, $Q_i(t)$, and is defined as being

$$Q_i(t) = \int_0^{\ell} w(x,t)\,Y_{i(x)}\,dx \tag{21}$$

The denominator of Equation 20 is called the generalized mass, $\mathcal{M}_i$, and is defined

$$\mathcal{M}_i = \int_0^{\ell} m(x)\,Y_{i(x)}^{\,2}\,dx \tag{22}$$

With these two definitions (Equations 21 and 22), the forcing function (Equation 18) can be written as

$$w(x,t) = \sum_i \frac{Q_i(t)}{\mathcal{M}_i}\,m(x)\,Y_{i(x)}^{\,2} \tag{23}$$

Now Equation 17 is integrated along the entire length of the vehicle and Equations 21 and 22 are substituted into the resulting expression. Dividing this expression by $\int_0^{\ell} m(x)\,Y_{i(x)}^{\,2}\,dx$, a set of simultaneous bending equations is obtained in the form

$$\ddot{\eta}_i + \frac{1}{\mathcal{M}_i}\int_0^{\ell}\frac{d^2}{dx^2}\left[E(x)I(x)\frac{\partial^2 Y_{i(x)}}{\partial x^2}\right]Y_{i(x)}\,dx\,\eta_i = \sum_i \frac{Q_i(t)}{\mathcal{M}_i(t)} \tag{24}$$

where the natural frequency of the i^{th} mode is defined as being

$$\omega_i^2 = \frac{1}{m_i} \int_0^l \frac{d}{dx} \left[E(x) I(x) \frac{\partial^2 Y_{i(x)}}{\partial x^2} \right] Y_{i(x)} \, dx \tag{25}$$

For all practical purposes, there are small dissipative forces in the system. However, the energy dissipated by these forces is small when compared with the elastic energy of the system. Therefore, the damping that these dissipative forces provide is very small. Since this damping does exist, it can be included in Equation 24 as the following shows:

$$\ddot{\eta}_i + 2\zeta_i \omega_i \dot{\eta}_i + \omega_i^2 \eta_i = \frac{Q_i(t)}{m_i} \tag{26}$$

where the damping ratio must be obtained from experimental data (See Table III).

2.3.2 Generalized Mass

A numerical value for the generalized mass (Equation 22) can be obtained by representing the mass of the system as the sum of a discrete number of lumped masses at stations along the x body axis of the vehicle. Knowing $Y_{i(x)}$, the integration of Equation 22 can be approximated by the following summation:

$$m_i = \sum_k m_{(x_k)} \, Y_{i(x_k)}^2 \tag{27}$$

where $m(x_k)$ is the lumped mass at station x_k. The accuracy of this method will depend on the number of lumped masses shown. Of course, graphical integration could be performed and more accurate results obtained. Values of m_i are tabulated in Table III for the first four bending modes.

2.3.3 Generalized Force

The generalized force resulting from external loading on the vehicle originates from a number of sources; namely,

1. control rocket thrust,
2. inertial forces of the gimballing rocket engines, and
3. aerodynamic forces.

Hence, the generalized force, $Q_i(t)$ (Equation 21), is the sum of the above three sources:

$$Q_i(t) = Q_{i_\beta}(t) + Q_{i_{\ddot{\beta}}}(t) + Q_{i_{AERO}}(t) \tag{28}$$

2.3.3.1 Control Rocket Thrust

The thrust of the control rockets is assumed concentrated at the gimbal point (i.e., station x_β). With this assumption, the lateral force which will cause bending is $R' \sin \beta_L$. Assuming that $\sin \beta_L \approx \beta_L$ (rad), the lateral force due to the control rocket thrust is $R' \beta_L$.

Substituting $R'\beta_L$ into Equation 21, the generalized force due to the control rockets, $Q_{i_\beta}(t)$, is

$$Q_{i_\beta}(t) = R' Y_{i(x_\beta)} \beta_L \tag{29}$$

Values for R' and $Y_{i\,(x_\beta)}$ can be obtained from Tables I and IV respectively ($R' = \frac{1}{2} F$).

2.3.3.2 Inertial Forces of Control Rocket Engines

The inertial forces due to gimballing the control rocket engines have already been obtained in Section 2.1. If this inertial force is substituted into Equation 21, the following generalized force is obtained:

$$Q_{i_{\ddot{\beta}}}(t) = 4\left[m_e(x_\beta - x_e)\, Y_{i_{(x_\beta)}} + I_e\, Y'_{i_{(x_\beta)}}\right]\ddot{\beta}_L \tag{30}$$

$Q_{i_{\ddot{\beta}}}(t)$ can be computed using the data in Tables II and IV.

2.3.3.3 Aerodynamic Forces

The normal force acting on the vehicle is usually given as a local normal force coefficient distribution ($\partial C_{z_\alpha} / \partial x$) along its length (see Figure 4). In order to obtain the total normal force derivative, it is necessary to integrate with respect to x along the entire length of the vehicle.

$$C_{z_\alpha} = \int_0^{l} \frac{\partial C_{z_\alpha}}{\partial x}\, dx \tag{31}$$

For this study, the normal force derivative was obtained by concentrating the normal force coefficients at certain intervals and solving for C_{z_α} as follows:

$$C_{z_\alpha} = \int_0^{l} \frac{\partial C_{z_\alpha}}{\partial x}\, dx = \sum_{n=1}^{N} C_{z_\alpha}(x_n) \tag{32}$$

where x_n is the station where the local normal force coefficient was concentrated. Now, the normal force due to angle of attack is

$$F_z = \bar{q} A \sum_{n=1}^{N} \frac{\partial C_{z_\alpha}}{\partial x} \Delta x_n\, \alpha \tag{33}$$

Substituting Equation 33 into Equation 21, the generalized force due to angle of attack, $Q_{i_\alpha}(t)$, is

$$Q_{i_\alpha}(t) = \bar{q} A \sum_{n=1}^{N} \frac{\partial C_{z_\alpha}}{\partial x} \Delta x_n\, \alpha\, Y_{i_{(x_n)}} \tag{34}$$

It should be noted that the following aerodynamic terms have been omitted:

1. the local change in angle of attack due to the bending of the vehicle,
2. the aerodynamic damping forces due to the angle of attack changes caused by the following local velocities which are normal to the aerodynamic velocity vector:
   a. rigid body angular velocity

$$\alpha_{\dot{\phi}} = -\frac{(x_n - x_{CG})}{V}\,\dot{\phi} \tag{35}$$

b. velocity of beam displacement

$$\alpha_{\dot{z}} = -\frac{\dot{z}}{V} = -\frac{1}{V}\sum_i Y_{i(x_n)}\dot{\eta}_i \tag{36}$$

2.4 ENGINE-ACTUATOR EQUATION

The dynamics of the engine and actuator were obtained from Reference 1 and are presented below.

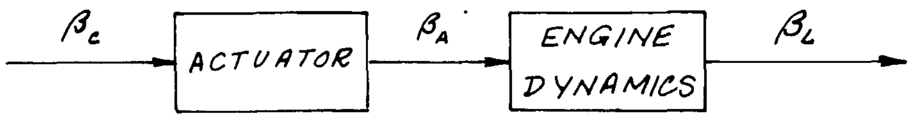

A detailed block diagram of Sketch D is shown in Figure 5. No numerical values were given for the expressions shown in Figure 5. However, Figures 6 and 7 were given along with the following equation:

$$\dddot{\beta}_L + 23.7\ddot{\beta}_L + 2259\dot{\beta}_L + 31,130\beta_L = 31,130\beta_c \tag{37}$$

2.5 BENDING MOMENT EQUATION

There are two methods used to calculate the bending moment at any station x_n:

1. mode-displacement method, and
2. mode-acceleration method.

For the mode-displacement method, the equation used in Reference 3 for obtaining the bending moment at station x_n is

$$BM(x_n) = E(x_n)\,I(x_n)\sum_i \frac{d^2 Y_{i(x_n)}}{dx_n^2}\eta_i \tag{38}$$

As noted in Reference 3, the mode-displacement method is not accurate when only a limited number of modes is included and when the mass distribution is highly discontinuous. Since only the first and second modes are currently being examined and the mass distribution is highly discontinuous, the mode-acceleration method is used. In Reference 3, the bending moment at any station (x_n) using the mode-acceleration method is obtained by summing the moments from the nose back along the vehicle to station x_n.

$$BM(x_n) = \sum_j \left\{ -m(x_j)\,a_z(x_j) + \bar{q}\,A\,C_{z_\alpha(x_j)}\left[\alpha + \sum_i Y'_{i(x_j)}\eta_i - \frac{1}{V}\sum_i Y_{i(x_j)}\dot{\eta}_i - \frac{1}{V}(x_j - x_{CG})\dot{\phi}\right]\right\}(x_j - x_n) \tag{39}$$

where j = index of stations forward of x_n, i = modal index, and n = station index.

Values for the coefficients of Equation 39 can be computed using the data in Tables I and IV and the data shown in Figures 4 and 8.

2.6 ACCELEROMETER EQUATION

Assuming no instrumentation dynamics (the frequency of the accelerometer dynamics is much higher than the modes of motion), the accelerometer equation at any station x_ϕ can be easily derived from Figure 2.

$$a_z = (x_\phi - x_{CG})\ddot{\phi} + (\bar{q} A C_{z_\alpha})\alpha + \sum_i Y_{i(x_\phi)} \ddot{\eta}_i - \sum_i \left\{ \frac{F}{m} Y'_{i(x_\phi)} - \frac{F-X}{m} Y'_{i(x_\phi)} \right\} \eta_i + \frac{R'}{m} \beta_L \tag{40}$$

2.7 POSITION AND RATE GYRO EQUATIONS

The equation for a position gyro can be readily derived for any station x_ϕ from Figure 2.

$$\phi_{PG} = \phi_{\substack{RIGID\\BODY}} - \sum_i Y'_{i(x_\phi)} \eta_i \tag{41}$$

The equation for the rate gyro (assuming no instrumentation dynamics) can be obtained by taking the derivative of Equation 41 with respect to time. Hence,

$$\dot{\phi}_{RG} = \dot{\phi}_{\substack{RIGID\\BODY}} - \sum_i Y'_{i(x_\phi)} \dot{\eta}_i \tag{42}$$

3.0 TRANSFER FUNCTIONS

3.1 RIGID BODY

Using the data from Reference 1 and Equations 1, 4 and 37, the following are obtained:

$$\ddot{\phi} - .0733\alpha + .000737\ddot{\beta}_L + .45\beta_L = 0 \tag{1}$$

$$-\dot{\phi} + .0405\phi + \dot{\alpha} + .01067\alpha + .02106\beta_L = 0 \tag{4}$$

$$\dddot{\beta}_L + 23.7\ddot{\beta}_L + 2259\dot{\beta}_L + 31,130\beta_L = 31,130\beta_c \tag{37}$$

Cramer's Rule was used to obtain the following transfer functions:

$$\frac{\phi}{\beta_c}(s) = \frac{-2.14\left(1+\frac{s}{.0141}\right)\left[1+\frac{2(.00007)}{24.71}s+\left(\frac{s}{24.71}\right)^2\right]}{D_R} \tag{42}$$

$$\frac{\alpha}{\beta_c}(s) = \frac{6.14\left(1-\frac{s}{.04042}\right)\left[1+\frac{2(.5777)}{24.73}s+\left(\frac{s}{24.73}\right)^2\right]}{D_R} \tag{43}$$

$$\frac{\beta_L}{\beta_c}(s) = \frac{\left(1+\frac{s}{.2942}\right)\left(1-\frac{s}{.2417}\right)\left(1-\frac{s}{.04175}\right)}{D_R} \tag{44}$$

where

$$D_R = \left(1+\frac{s}{.2942}\right)\left(1+\frac{s}{14.64}\right)\left(1-\frac{s}{.2417}\right)\left(1-\frac{s}{.04175}\right)\left[1+\frac{2(.098)}{46.11}s+\left(\frac{s}{46.11}\right)^2\right]$$

In order to reduce the complexity of the system equations, the following simplifications were incorporated in Equations 1 and 37. Since the mass and inertia of the gimballed engines are small when compared with the mass and inertia of the total vehicle, the coefficient

$$4\left[\frac{(x_{cg}-x_\beta)m_e(x_\beta-x_e)+I_e}{I_y}\right]$$

was assumed to be zero (m_e/m_{TOTAL} = .014 and $I_e/I_y = 55 \times 10^{-6}$). As a result of this simplification, a pair of zeros at a frequency of 24.7 rad/sec are discarded. These zeros are commonly called the "tail-wags-dog" zeros and occur at the frequency at which the inertial forces (discussed in Section 2.1) resulting from the gimballing of the control engines cancel the component of thrust normal to the missile axis due to deflection of the engine chambers. Their effect on the rigid body mode is minor.

The second simplification involves replacing Equation 37 with the following first-order equation:

$$\dot{\beta}_L + 17.9\beta_L = 17.9\beta_c \tag{45}$$

This simplification reduces the order of the system by two. The frequency of the discarded poles is 46.11 rad/sec. As can be seen from Table III, this frequency is well above the frequency range of interest. The real pole was moved from s = -14.64 to s = -17.9 in order to give a better representation of the magnitude and phase of the engine-actuator dynamics at the lower frequencies (see Figures 6 and 7).

The third simplification assumes that $4 \frac{F-X}{m} \frac{m_e(x_\beta - x_e)}{I_y}$ in the pitch acceleration equation is zero. This assumption is valid because the pitch acceleration due to moving the mass of the engine is negligible when compared with the pitch acceleration due to the control rockets, i.e.,

$$\frac{R'(x_{CG} - x_\beta)}{I_y} >>>> 4 \frac{F-X}{m} \frac{m_e(x_\beta - x_e)}{I_y}$$

With the above simplifications incorporated into the above equations, the rigid body system equations are:

$$\ddot{\phi} - .0733\alpha + .45\beta_L = 0 \qquad (46)$$

$$-\dot{\phi} + .0405\phi + \dot{\alpha} + .01067\alpha + .02106\beta_L = 0 \qquad (4)$$

$$\dot{\beta}_L + 17.9\beta_L = 17.9\beta_c \qquad (45)$$

The resulting simplified transfer functions are:

$$\frac{\phi}{\beta_c}(s) = \frac{-2.14\left(1 + \frac{s}{.0141}\right)}{D_R} \qquad (47)$$

$$\frac{\alpha}{\beta_c}(s) = \frac{6.14\left(1 - \frac{s}{.0404}\right)\left(1 + \frac{s}{21.41}\right)}{D_R} \qquad (48)$$

$$\frac{\beta_L}{\beta_c}(s) = \frac{\left(1 + \frac{s}{.2942}\right)\left(1 - \frac{s}{.2417}\right)\left(1 - \frac{s}{.04175}\right)}{D_R} \qquad (49)$$

where

$$D_R = \left(1 + \frac{s}{.2942}\right)\left(1 - \frac{s}{.2417}\right)\left(1 - \frac{s}{.04175}\right)\left(1 + \frac{s}{17.9}\right)$$

Using the data in Table I, the accelerometer equations at the following stations are:

$x_\phi = 22.7 \qquad a_z = -18.8\ddot{\phi} + 5.54\alpha + 10.93\beta_L$

x_ϕ = 41.5 $\quad a_z = 5.54\alpha + 10.93\beta_L$

x_ϕ = 55.4 $\quad a_z = 13.9\ddot{\phi} + 5.54\alpha + 10.93\beta_L$

x_ϕ = 92.1 $\quad a_z = 50.6\ddot{\phi} + 5.54\alpha + 10.93\beta_L$

x_ϕ = 122.4 $\quad a_z = 80.9\ddot{\phi} + 5.54\alpha + 10.93\beta_L$

In order to use a_z in the synthesis of the control law (see Reference 4), it is necessary to make a_z a function of α and β_L. Therefore, $\ddot{\phi}$ can be replaced with the pitch acceleration equation (46). Hence,

$$a_z = (x_\phi - x_{CG})(.0733\alpha - .45\beta_L) + 5.54\alpha + 10.93\beta_L \tag{50}$$

Now, at the following stations, the accelerometer equations are:

x_ϕ = 22.7 $\quad a_z = 4.16\alpha + 19.38\beta_L$

x_ϕ = 41.5 $\quad a_z = 5.54\alpha + 10.93\beta_L$

x_ϕ = 55.4 $\quad a_z = 6.56\alpha + 4.68\beta_L$

x_ϕ = 92.1 $\quad a_z = 9.25\alpha - 11.82\beta_L$

x_ϕ = 122.4 $\quad a_z = 11.47\alpha - 25.47\beta_L$

3.2 FIRST AND SECOND BENDING MODES

Substituting the data from Reference 1 into the system equations, the following are obtained:

$$\ddot{\phi} - .0733\alpha - .01067\eta_1 - .02197\eta_2 + .000737\ddot{\beta}_L + .45\beta_L = 0 \tag{1}$$

$$-\dot{\phi} + .0405\phi + \dot{\alpha} + .01067\alpha - .000751\ddot{\eta}_1 - .0015\eta_1 - .001\ddot{\eta}_2 - .002\eta_2 + .02106\beta_L = 0 \tag{4}$$

$$-5.4532\alpha + \ddot{\eta}_1 + .02317\dot{\eta}_1 + 5.37\eta_1 - .027\ddot{\beta}_L - 15.83\beta_L = 0 \tag{26}$$
(First Mode)

$$-2.36\alpha + \ddot{\eta}_2 + .05642\dot{\eta}_2 + 31.8\eta_2 - .040\ddot{\beta}_L - 22.77\beta_L = 0 \tag{26}$$
(Second Mode)

$$\dddot{\beta}_L + 23.7\ddot{\beta}_L + 2259\dot{\beta}_L + 31{,}130\beta_L = 31{,}130\beta_C \tag{37}$$

Transforming the above equations into the s-domain and applying Cramer's Rule, the following transfer functions are obtained:

$$\frac{\phi}{\beta_c}(s) = \frac{-1.357\left(1+\frac{s}{.01171}\right)\left[1+\frac{2(.00049)}{24.71}s+\left(\frac{s}{24.71}\right)^2\right]\left[1+\frac{2(.0047)}{5.542}s+\left(\frac{s}{5.542}\right)^2\right]\left[1+\frac{2(.0043)}{2.231}s+\left(\frac{s}{2.231}\right)^2\right]}{D_{B_2}} \tag{51}$$

$$\frac{\alpha}{\beta_c}(s) = \frac{4.69\left(1-\frac{s}{.04044}\right)\left(1+\frac{s}{20.19}\right)\left[1+\frac{2(.028)}{2.235}s+\left(\frac{s}{2.235}\right)^2\right]\left[1+\frac{2(.13)}{5.422}s+\left(\frac{s}{5.422}\right)^2\right]\left[1+\frac{2(.183)}{19.36}s+\left(\frac{s}{19.36}\right)^2\right]}{D_{B_2}} \tag{52}$$

$$\frac{\eta_1}{\beta_c}(s) = \frac{7.71\left(1-\frac{s}{.0408}\right)\left(1+\frac{s}{.4948}\right)\left(1-\frac{s}{.4502}\right)\left[1+\frac{2(.00545)}{5.639}s+\left(\frac{s}{5.639}\right)^2\right]\left[1+\frac{2(.00015)}{24.21}s+\left(\frac{s}{24.21}\right)^2\right]}{D_{B_2}} \tag{53}$$

$$\frac{\eta_2}{\beta_c}(s) = \frac{1.061\left(1+\frac{s}{.5583}\right)\left[1+\frac{2(.00027)}{23.86}s+\left(\frac{s}{23.86}\right)^2\right]\left[1+\frac{2(.0062)}{2.317}s+\left(\frac{s}{2.317}\right)^2\right]\left[1-\frac{2(.6514)}{.4289}s+\left(\frac{s}{.4289}\right)^2\right]}{D_{B_2}} \tag{54}$$

$$\frac{\beta_L}{\beta_c}(s) = \frac{\left(1-\frac{s}{.04158}\right)\left(1+\frac{s}{.3145}\right)\left(1-\frac{s}{.2641}\right)\left[1+\frac{2(.0048)}{5.637}s+\left(\frac{s}{5.637}\right)^2\right]\left[1+\frac{2(.0044)}{2.326}s+\left(\frac{s}{2.326}\right)^2\right]}{D_{B_2}} \tag{55}$$

where

$$D_{B_2} = \left(1-\frac{s}{.04158}\right)\left(1+\frac{s}{.3145}\right)\left(1-\frac{s}{.2641}\right)\left[1+\frac{2(.0048)}{5.637}s+\left(\frac{s}{5.637}\right)^2\right]\left[1+\frac{2(.0044)}{2.326}s+\left(\frac{s}{2.326}\right)^2\right] \times \left(1+\frac{s}{14.62}\right)\left[1+\frac{2(.098)}{46.1}s+\left(\frac{s}{46.1}\right)^2\right] \tag{56}$$

The complexity of the system equations with bending modes can be reduced by incorporating the three simplifications presented in Section 3.1. Also, Z and the pitch accelerations due to bending are small and have a negligible effect on the location of the poles and zeros. Hence, the following terms are considered zero:

$$\sum_i \left\{ \frac{F}{I_y} Y_{i(x_\beta)} - \frac{F(x_{CG}-x_\beta)}{I_y} Y'_{i(x_\beta)} - 4\,\frac{F-X}{m}\,\frac{m_e(x_\beta - x_e)}{I_y} Y'_{i(x_\beta)} \right\} = 0$$

$$\frac{F}{mV}\sum_i Y'_{i(x_\beta)} = 0$$

The engine mass and inertia terms of the generalized forcing function in the bending equations may be neglected because they are small compared with the total mass and inertia of the vehicle. Therefore, assume

$$\frac{4}{m_i}\left\{ m_e(x_\beta - x_e) Y_{i(x_\beta)} + I_e Y'_{i(x_\beta)} \right\} = 0$$

The resulting simplified system equations with the first and second bending modes are:

$$\ddot{\phi} - .0733\alpha + .45\beta_L = 0 \tag{57}$$

$$-\dot{\phi} + .0405\phi + \dot{\alpha} + .01067\alpha + .02106\beta_L = 0 \tag{58}$$

$$-5.4532\alpha + \ddot{\eta}_1 + .02317\dot{\eta}_1 + 5.37\eta_1 - 15.83\beta_L = 0 \tag{59}$$

$$-2.36\alpha + \ddot{\eta}_2 + .05642\,\dot{\eta}_2 + 31.8\,\eta_2 - 22.77\beta_L = 0 \quad (60)$$

$$\dot{\beta}_L + 17.9\,\beta_L = 17.9\beta_C \quad (45)$$

The resulting transfer functions are:

$$\frac{\phi}{\beta_C}(s) = \frac{-2.14\left(1+\frac{s}{.0141}\right)\left[1+\frac{2(.005)}{2.317}s+\left(\frac{s}{2.317}\right)^2\right]\left[1+\frac{2(.005)}{5.639}s+\left(\frac{s}{5.639}\right)^2\right]}{D_{B_2}} \quad (61)$$

$$\frac{\alpha}{\beta_C}(s) = \frac{6.14\left(1-\frac{s}{.0404}\right)\left(1+\frac{s}{21.41}\right)\left[1+\frac{2(.005)}{2.317}s+\left(\frac{s}{2.317}\right)^2\right]\left[1+\frac{2(.005)}{5.639}s+\left(\frac{s}{5.639}\right)^2\right]}{D_{B_2}} \quad (62)$$

$$\frac{\eta_1}{\beta_C}(s) = \frac{9.18\left(1-\frac{s}{.0408}\right)\left(1-\frac{s}{.4543}\right)\left(1+\frac{s}{.4986}\right)\left[1+\frac{2(.005)}{5.639}s+\left(\frac{s}{5.639}\right)^2\right]}{D_{B_2}} \quad (63)$$

$$\frac{\eta_2}{\beta_C}(s) = \frac{1.17\left(1-\frac{s}{.0412}\right)\left(1-\frac{s}{.3194}\right)\left(1+\frac{s}{.3691}\right)\left[1+\frac{2(.005)}{2.317}s+\left(\frac{s}{2.317}\right)^2\right]}{D_{B_2}} \quad (64)$$

$$\frac{\beta_L}{\beta_C}(s) = \frac{\left(1-\frac{s}{.04175}\right)\left(1-\frac{s}{.2417}\right)\left(1+\frac{s}{.2942}\right)\left[1+\frac{2(.005)}{2.317}s+\left(\frac{s}{2.317}\right)^2\right]\left[1+\frac{2(.005)}{5.639}s+\left(\frac{s}{5.639}\right)^2\right]}{D_{B_2}} \quad (65)$$

where

$$D_{B_2}(s) = \left(1+\frac{s}{17.9}\right)\left(1+\frac{s}{.2942}\right)\left(1-\frac{s}{.2417}\right)\left(1-\frac{s}{.04175}\right)\left[1+\frac{2(.005)}{5.639}s+\left(\frac{s}{5.639}\right)^2\right]\left[1+\frac{2(.005)}{2.317}s+\left(\frac{s}{2.317}\right)^2\right]$$

In order to use a_z in the synthesis of a control law which includes η_1 and η_2, it is necessary to make a_z (40) a function of $\dot{\phi}$, ϕ, $\dot{\alpha}$, α, $\dot{\eta}_1$, η_1, $\dot{\eta}_2$, η_2, and β_L. $\ddot{\phi}$ can be replaced with the simplified pitch acceleration equation (57). $\ddot{\eta}_1$ can be obtained from the first bending mode equation (59), and $\ddot{\eta}_2$ can be obtained from the second bending mode equation (60). Hence,

$$a_z = (x_\phi - x_{CG})\ddot{\phi} + 5.54\alpha + Y_{1(x_\phi)}\ddot{\eta}_1 - (.78 - 21.05\,Y'_{1(x_\phi)})\eta_1 + Y_{2(x_\phi)}\ddot{\eta}_2 - (1.042 - 21.05\,Y'_{2(x_\phi)})\eta_2 + 10.93\beta_L \quad (40)$$

where

$$\ddot{\phi} = .0733\alpha - .45\beta_L \quad (57)$$

$$\ddot{\eta}_1 = 5.4532\alpha - .02317\,\dot{\eta}_1 - 5.37\eta_1 + 15.83\beta_L \quad (59)$$

$$\ddot{\eta}_2 = 2.36\alpha - .05642\,\dot{\eta}_2 - 31.8\eta_2 + 22.77\beta_L \quad (60)$$

Using the data in Table IV, the accelerometer equation is computed for five stations:

$$x_\phi = 22.7 \qquad a_z = 5.0402\,\alpha - .00463\,\dot{\eta}_1 - 1.12\,\eta_1 - .05078\,\dot{\eta}_2 + 2.809\,\eta_2 + 20.507\,\beta_L$$

$$x_\phi = 41.7 \qquad a_z = 2.1035\,\alpha + .009036\,\dot{\eta}_1 + 1.903\,\eta_1 + .0313\,\dot{\eta}_2 + 16.786\,\eta_2 - 7.88\,\beta_L$$

$$x_\phi = 55.4 \qquad a_z = 1.484\,\alpha + .0168\,\dot{\eta}_1 + 3.479\,\eta_1 + .0268\,\dot{\eta}_2 + 13.622\,\eta_2 - 17.618\,\beta_L$$

$$x_\phi = 92.1 \qquad a_z = 9.779\,\alpha + .01158\,\dot{\eta}_1 + \eta_1 + .07786\,\dot{\eta}_2 - 45.745\,\eta_2 + 11.668\,\beta_L$$

$$x_\phi = 122.4 \qquad a_z = 23.2638\,\alpha - .0468\,\dot{\eta}_1 - 14.207\,\eta_1 - .01862\,\dot{\eta}_2 - 8.568\,\eta_2 + 14.016\,\beta_L$$

3.3 FIRST FOUR BENDING MODES

Using the simplifications of Section 3.3, the system equations with four bending modes are:

$$\ddot{\phi} - .0733\,\alpha + .45\,\beta_L = 0 \tag{57}$$

$$-\dot{\phi} + .0405\,\phi + \dot{\alpha} + .01067\,\alpha + .02106\,\beta_L = 0 \tag{58}$$

$$-5.4532\,\alpha + \ddot{\eta}_1 + .02317\,\dot{\eta}_1 + 5.37\,\eta_1 - 15.83\,\beta_L = 0 \tag{59}$$

$$-2.36\,\alpha + \ddot{\eta}_2 + .05642\,\dot{\eta}_2 + 31.8\,\eta_2 - 22.77\,\beta_L = 0 \tag{60}$$

$$-11.8\,\alpha + \ddot{\eta}_3 + .0918\,\dot{\eta}_3 + 84.25\,\eta_3 - 26.25\,\beta_L = 0 \tag{66}$$

$$1.336\,\alpha + \ddot{\eta}_4 + .125\,\dot{\eta}_4 + 156.2\,\eta_4 - 4.48\,\beta_L = 0 \tag{67}$$

The resulting transfer functions are:

$$\frac{\phi}{\beta_C}(s) = \frac{-2.14\left(1+\frac{s}{.0141}\right)\left[1+\frac{2(.005)}{2.317}s+\left(\frac{s}{2.317}\right)^2\right]\left[1+\frac{2(.005)}{5.639}s+\left(\frac{s}{5.639}\right)^2\right]\left[1+\frac{2(.005)}{9.179}s+\left(\frac{s}{9.179}\right)^2\right]\left[1+\frac{2(.005)}{12.5}s+\left(\frac{s}{12.5}\right)^2\right]}{D_{B_4}} \tag{68}$$

$$\frac{\alpha}{\beta_c}(s) = \frac{6.14\left(1-\frac{s}{.0404}\right)\left(1+\frac{s}{21.41}\right)\left[1+\frac{2(.005)}{2.317}s+\left(\frac{s}{2.317}\right)^2\right]\left[1+\frac{2(.005)}{5.639}s+\left(\frac{s}{5.639}\right)^2\right]\left[1+\frac{2(.005)}{9.179}s+\left(\frac{s}{9.179}\right)^2\right]\left[1+\frac{2(.006)}{12.5}s+\left(\frac{s}{12.5}\right)^2\right]}{D_{B_4}} \tag{69}$$

$$\frac{\eta_1}{\beta_c}(s) = \frac{9.18\left(1-\frac{s}{.0408}\right)\left(1-\frac{s}{.4543}\right)\left(1+\frac{s}{.4986}\right)\left[1+\frac{2(.005)}{5.639}s+\left(\frac{s}{5.639}\right)^2\right]\left[1+\frac{2(.005)}{9.179}s+\left(\frac{s}{9.179}\right)^2\right]\left[1+\frac{2(.005)}{12.5}s+\left(\frac{s}{12.5}\right)^2\right]}{D_{B_4}} \tag{70}$$

$$\frac{\eta_2}{\beta_c}(s) = \frac{1.17\left(1-\frac{s}{.0412}\right)\left(1-\frac{s}{.3194}\right)\left(1+\frac{s}{.3691}\right)\left[1+\frac{2(.005)}{2.317}s+\left(\frac{s}{2.317}\right)^2\right]\left[1+\frac{2(.005)}{9.179}s+\left(\frac{s}{9.179}\right)^2\right]\left[1+\frac{2(.005)}{12.5}s+\left(\frac{s}{12.5}\right)^2\right]}{D_{B_4}} \tag{71}$$

$$\frac{\eta_3}{\beta_c}(s) = \frac{1.17\left(1-\frac{s}{.04075}\right)\left(1-\frac{s}{.5028}\right)\left(1+\frac{s}{.5447}\right)\left[1+\frac{2(.005)}{2.317}s+\left(\frac{s}{2.317}\right)^2\right]\left[1+\frac{2(.005)}{5.639}s+\left(\frac{s}{5.639}\right)^2\right]\left[1+\frac{2(.005)}{12.5}s+\left(\frac{s}{12.5}\right)^2\right]}{D_{B_4}} \tag{72}$$

$$\frac{\eta_4}{\beta_c}(s) = \frac{-.0238\left(1-\frac{s}{.0391}\right)\left[1+\frac{2(.112)}{.2512}s+\left(\frac{s}{.2512}\right)^2\right]\left[1+\frac{2(.005)}{2.317}s+\left(\frac{s}{2.317}\right)^2\right]\left[1+\frac{2(.005)}{5.639}s+\left(\frac{s}{5.639}\right)^2\right]\left[1+\frac{2(.005)}{9.179}s+\left(\frac{s}{9.179}\right)^2\right]}{D_{B_4}} \tag{73}$$

$$\frac{\beta_L}{\beta_c}(s) = \frac{\left(1-\frac{s}{.04175}\right)\left(1+\frac{s}{.2942}\right)\left(1-\frac{s}{.2417}\right)\left[1+\frac{2(.005)}{2.317}s+\left(\frac{s}{2.317}\right)^2\right]\left[1+\frac{2(.005)}{5.639}s+\left(\frac{s}{5.639}\right)^2\right]\left[1+\frac{2(.005)}{9.179}s+\left(\frac{s}{9.179}\right)^2\right]\left[1+\frac{2(.005)}{12.5}s+\left(\frac{s}{12.5}\right)^2\right]}{D_{B_4}} \tag{74}$$

where

$$D_{B_4}(s) = \left(1-\frac{s}{.04175}\right)\left(1-\frac{s}{.2417}\right)\left(1+\frac{s}{17.9}\right)\left(1+\frac{s}{.2942}\right)\left[1+\frac{2(.005)}{2.317}s+\left(\frac{s}{2.317}\right)^2\right]\left[1+\frac{2(.005)}{5.639}s+\left(\frac{s}{5.639}\right)^2\right]\left[1+\frac{2(.005)}{9.179}s+\left(\frac{s}{9.179}\right)^2\right]\left[1+\frac{2(.005)}{12.5}s+\left(\frac{s}{12.5}\right)^2\right]$$

4.0 APPLICATION OF OPTIMAL CONTROL THEORY TO CONTROL A HIGHLY ELASTIC VEHICLE

The technique presented in this section is the same as shown in Reference 4. Rynaski in Reference 4 denotes that the objective of linear optimal design is to provide a system that will give a rapid and smooth response to a disturbance or a command input, guarantee system stability, and increase the damping of the bending modes.

4.1 PERFORMANCE INDEX AND CLOSED-LOOP POLES

The equations of motion (57, 58, 59, 60, 45) with the first and second bending modes are rewritten below in first-order form:

$$\begin{bmatrix} \dot{\phi} \\ \ddot{\phi} \\ \dot{\alpha} \\ \dot{\eta}_1 \\ \ddot{\eta}_1 \\ \dot{\eta}_2 \\ \ddot{\eta}_2 \\ \dot{\beta}_L \end{bmatrix} = \begin{bmatrix} 0 & 1 & 0 & 0 & 0 & 0 & 0 & 0 \\ 0 & 1 & .0733 & 0 & 0 & 0 & 0 & -.45 \\ -.0405 & 0 & -.0107 & 0 & 0 & 0 & 0 & -.0211 \\ 0 & 0 & 0 & 0 & 1 & 0 & 0 & 0 \\ 0 & 0 & 5.45 & -5.37 & -.0563 & 0 & 0 & 15.83 \\ 0 & 0 & 0 & 0 & 0 & 0 & 1 & 0 \\ 0 & 0 & 2.36 & 0 & 0 & -31.8 & -.0564 & 22.77 \\ 0 & 0 & 0 & 0 & 0 & 0 & 0 & -17.9 \end{bmatrix} \begin{bmatrix} \phi \\ \dot{\phi} \\ \alpha \\ \eta_1 \\ \dot{\eta}_1 \\ \eta_2 \\ \dot{\eta}_2 \\ \beta_L \end{bmatrix} + \begin{bmatrix} 0 \\ 0 \\ 0 \\ 0 \\ 0 \\ 0 \\ 0 \\ 17.9 \end{bmatrix} \beta_c \qquad \text{(75) (a-h)}$$

or

$$\dot{x} = Fx + Gu \qquad y = Hx \qquad (76)$$

The performance index chosen is

$$2V = \int_0^\infty (q_1 \phi^2 + q_2 \eta_2^2 + q_3 \eta_1^2 + r\beta_c^2)\,dt \qquad (77)$$

The dynamic variables η_1 and η_2 are included in the performance index because they are directly associated with the bending mode motion. In Reference 5, the multivariable root square locus expression

$$\left| I + R^{-1} G' [-Is - F']^{-1} H'QH [Is - F]^{-1} G \right| = 0 \qquad (78)$$

gives the closed-loop poles as a function of the weighting factors (q_i) of the performance index.

I is an identity matrix
H is a matrix of numbers that defines the output of the system,
Q is a matrix of weighting factors of the performance index.

For this problem,

$$H = \begin{bmatrix} 1 & 0 & 0 & 0 & 0 & 0 & 0 & 0 \\ 0 & 0 & 0 & 1 & 0 & 0 & 0 & 0 \\ 0 & 0 & 0 & 0 & 0 & 1 & 0 & 0 \end{bmatrix} \tag{79}$$

$$Q = \begin{bmatrix} q_1 & 0 & 0 \\ 0 & q_2 & 0 \\ 0 & 0 & q_3 \end{bmatrix} \tag{80}$$

$$I = [1] \tag{81}$$

and

$$R^{-1} = \frac{1}{r} \tag{82}$$

In Equation 78,

$$H[Is-F]^{-1}G = \begin{bmatrix} \frac{\phi}{\beta_c}(s) \\ \frac{\eta_1}{\beta_c}(s) \\ \frac{\eta_2}{\beta_c}(s) \end{bmatrix} \tag{83}$$

and

$$G'[-Is-F']H' = \begin{bmatrix} \frac{\phi}{\beta_c}(-s) & \frac{\eta_1}{\beta_c}(-s) & \frac{\eta_2}{\beta_c}(-s) \end{bmatrix} \tag{84}$$

Therefore,

$$R^{-1}G'[-Is-F']^{-1}H'QH[Is-F]^{-1}G = -I \tag{85}$$

or

$$\frac{1}{r}\begin{bmatrix} \frac{\phi}{\beta_c}(-s) & \frac{\eta_1}{\beta_c}(-s) & \frac{\eta_2}{\beta_c}(-s) \end{bmatrix} \begin{bmatrix} q_1 & 0 & 0 \\ 0 & q_2 & 0 \\ 0 & 0 & q_3 \end{bmatrix} \begin{bmatrix} \frac{\phi}{\beta_c}(s) \\ \frac{\eta_1}{\beta_c}(s) \\ \frac{\eta_2}{\beta_c}(s) \end{bmatrix} = -1 \tag{86}$$

Expanding Equation 86, the following is obtained:

$$\frac{q_1}{r}\frac{\phi}{\beta_c}(s)\frac{\phi}{\beta_c}(-s)+\frac{q_3}{r}\frac{\eta_1}{\beta_c}(s)\frac{\eta_1}{\beta_c}(-s)+\frac{q_2}{r}\frac{\eta_2}{\beta_c}(s)\frac{\eta_2}{\beta_c}(-s)=-1$$

Therefore Equation 78 is

$$1+\frac{q_1}{r}\frac{\phi}{\beta_c}(s)\frac{\phi}{\beta_c}(-s)+\frac{q_3}{r}\frac{\eta_1}{\beta_c}(s)\frac{\eta_1}{\beta_c}(-s)+\frac{q_2}{r}\frac{\eta_2}{\beta_c}(s)\frac{\eta_2}{\beta_c}(-s)=0 \qquad (87)$$

where

$\frac{\phi}{\beta_c}(s)$ is the pitch angle transfer function (61)

$\frac{\eta_1}{\beta_c}(s)$ is the first bending mode variable transfer function (63)

$\frac{\eta_2}{\beta_c}(s)$ is the second bending mode variable transfer function (64)

To make a root square locus plot, it is desirable to put Equation 87 in root locus form. First, multiply and divide the third and fourth terms of Equation 87 by:

$$\frac{q_2}{r}\frac{\eta_2}{\beta_c}(s)\frac{\eta_2}{\beta_c}(-s)$$

Hence,

$$1+\frac{q_1}{r}\frac{\phi}{\beta_c}(s)\frac{\phi}{\beta_c}(-s)+\frac{q_2}{r}\frac{\eta_2}{\beta_c}(s)\frac{\eta_2}{\beta_c}(-s)\left[1+\frac{\frac{q_3}{r}\frac{\eta_1}{\beta_c}(s)\frac{\eta_1}{\beta_c}(-s)}{\frac{q_2}{r}\frac{\eta_2}{\beta_c}(s)\frac{\eta_2}{\beta_c}(-s)}\right]=0 \qquad (88)$$

Now multiply and divide Equation 88 by

$$\frac{q_1}{r}\frac{\phi}{\beta_c}(s)\frac{\phi}{\beta_c}(-s)$$

Hence,

$$1+\frac{q_1}{r}\frac{\phi}{\beta_c}(s)\frac{\phi}{\beta_c}(-s)\left\{1+\frac{\frac{q_2}{r}\frac{\eta_2}{\beta_c}(s)\frac{\eta_2}{\beta_c}(-s)}{\frac{q_1}{r}\frac{\phi}{\beta_c}(s)\frac{\phi}{\beta_c}(-s)}\left[1+\frac{\frac{q_3}{r}\frac{\eta_1}{\beta_c}(s)\frac{\eta_1}{\beta_c}(-s)}{\frac{q_2}{r}\frac{\eta_2}{\beta_c}(s)\frac{\eta_2}{\beta_c}(-s)}\right]\right\}=0 \qquad (89)$$

In order to obtain the closed-loop poles of the system, three root loci must be plotted. The first root locus is given by

$$1+\frac{\frac{q_3}{r}\frac{\eta_1}{\beta_c}(s)\frac{\eta_1}{\beta_c}(-s)}{\frac{q_2}{r}\frac{\eta_2}{\beta_c}(s)\frac{\eta_2}{\beta_c}(-s)}=0 \qquad (90)$$

Substituting Equations 63 and 64 into Equation 90 yields the following expression:

$$1+\frac{q_3}{q_2}\,\frac{(9.18)^2\left(1\pm\frac{s}{.0408}\right)\left(1\pm\frac{s}{.4543}\right)\left(1\pm\frac{s}{.4986}\right)\left[1\pm\frac{2(.005)}{5.639}s+\left(\frac{s}{5.639}\right)^2\right]}{(1.17)^2\left(1\pm\frac{s}{.0412}\right)\left(1\pm\frac{s}{.3194}\right)\left(1\pm\frac{s}{.3691}\right)\left[1\pm\frac{2(.005)}{2.317}s+\left(\frac{s}{2.317}\right)^2\right]}=0 \qquad (91)$$

The first locus is shown in Figure 9. The maximum damping ratio was obtained at $q_3/q_2 = 0.5$. The second locus is given by:

$$1 + \frac{q_2}{q_1}\left[\frac{K_{\eta_2}^{\,2} \frac{q_3}{q_2} K_{\eta_1}^{\,2}}{K_\phi^{\,2}}\right]\left[\frac{\text{roots from Fig. 9 when } q_3/q_2 = .5}{N_\phi \bar{N}_\phi}\right] = 0 \qquad (92)$$

where

$$\frac{\eta_1}{\beta_c}(s)\,\frac{\eta_1}{\beta_c}(-s) = K_{\eta_1}^{\,2}\,\frac{N_{\eta_1}\bar{N}_{\eta_1}}{D\bar{D}}$$

$$\frac{\eta_2}{\beta_c}(s)\,\frac{\eta_2}{\beta_c}(-s) = K_{\eta_2}^{\,2}\,\frac{N_{\eta_2}\bar{N}_{\eta_2}}{D\bar{D}}$$

$$\frac{\phi}{\beta_c}(s)\,\frac{\phi}{\beta_c}(-s) = K_\phi^{\,2}\,\frac{N_\phi\bar{N}_\phi}{D\bar{D}}$$

Hence, Equation 92 is

$$1 + \frac{\frac{q_2}{q_1}\left[\frac{(1.17)^2 + 0.5(9.18)^2}{(-2.14)^2}\right]\left[1 \pm \frac{2(.39)}{3.92}s + \left(\frac{s}{3.92}\right)^2\right]\left[1 \pm \frac{2(.99)}{.47}s + \left(\frac{s}{.47}\right)^2\right]}{\left(1 \pm \frac{s}{.014}\right)\left[1 \pm \frac{2(.005)}{2.317}s + \left(\frac{s}{2.317}\right)^2\right]\left[1 \pm \frac{2(.005)}{5.639}s + \left(\frac{s}{5.639}\right)^2\right]} = 0$$

The second locus is shown in Figure 10. The roots for a gain $q_2/q_1 = 4$ are used for the third locus so that the pole originating from the open-loop rigid body pole will be at a frequency that is less than 1 rad/sec. Also, for greater values of q_2/q_1 the bending mode damping may not be obtainable.

The third locus describes the closed-loop poles of the optimal system and is given by

$$1 + \frac{\frac{q_1}{r}\left[K_\phi^{\,2} + \frac{q_2}{q_1}K_{\eta_2}^{\,2} + \frac{q_3}{q_2}K_{\eta_1}^{\,2}\right]\left[\text{roots from Fig. 10 when } q_2/q_1 = 4.0\right]}{D(s)\;D(-s)} \qquad (93)$$

Hence Equation 93 is

$$1 + \frac{\frac{q_1}{r}\left[(-2.14)^2 + 4(1.17)^2 + .5(9.18)^2\right]\left(1 \pm \frac{s}{.0825}\right)\left[1 \pm \frac{2(.43)}{2.47}s + \left(\frac{s}{2.47}\right)^2\right]\left[1 \pm \frac{2(.375)}{5.6}s + \left(\frac{s}{5.6}\right)^2\right]}{\left(1 \pm \frac{s}{17.9}\right)\left(1 \pm \frac{s}{.2942}\right)\left(1 \pm \frac{s}{.2417}\right)\left(1 \pm \frac{s}{.04175}\right)\left[1 \pm \frac{2(.005)}{5.639}s + \left(\frac{s}{5.639}\right)^2\right]\left[1 \pm \frac{2(.005)}{2.317}s + \left(\frac{s}{2.317}\right)^2\right]}$$

The third locus is shown in Figure 11. From Figure 11, it can be seen that good damping of the first two bending modes can be obtained using linear optimal analysis techniques. By observing Figure 11, a desirable level of damping can be chosen for a value of q_1/r. For example, choose $q_1/r = 20$ and let r = 1. Then

$$q_1 = 20$$
$$q_2 = 80$$
$$q_3 = 40$$

and the performance index becomes

$$2V = \int_0^\infty (20\phi^2 + 80\eta_{l_2}^{\,2} + 40\eta_{l_1}^{\,2} + \beta_c^{\,2})dt \tag{94}$$

The closed-loop poles are

$$\Delta(s) = \left(1+\frac{s}{.0825}\right)\left(1+\frac{s}{17.91}\right)\left[1+\frac{2(.75)}{1.09}s+\left(\frac{s}{1.09}\right)^2\right]\left[1+\frac{2(.1)}{2.4}s+\left(\frac{s}{2.4}\right)^2\right]\left[1+\frac{2(.01)}{5.64}s+\left(\frac{s}{5.64}\right)^2\right] \tag{95}$$

4.2 FEEDBACK GAINS AND OPTIMAL CONTROL LAW

The optimal control law is of the form

$$u = -Kx \tag{96}$$

and the closed-loop optimal system becomes

$$\dot{x} = (F - GK)x \tag{97}$$

and the characteristic equation is

$$|Is - F + GK| = 0 \tag{98}$$

where

$$K = \begin{bmatrix} K_1 & K_2 & K_3 & K_4 & K_5 & K_6 & K_7 & K_8 \end{bmatrix}$$

Equation 98 is then

$$\begin{vmatrix} s & -1 & 0 & 0 & 0 & 0 & 0 & 0 \\ 0 & s & -.0733 & 0 & 0 & 0 & 0 & .45 \\ .0405 & -1 & s+.0107 & 0 & 0 & 0 & 0 & .0211 \\ 0 & 0 & 0 & s & -1 & 0 & 0 & 0 \\ 0 & 0 & -5.45 & 5.37 & s+.0563 & 0 & 0 & -15.83 \\ 0 & 0 & 0 & 0 & 0 & s & -1 & 0 \\ 0 & 0 & -2.36 & 0 & 0 & 31.8 & s+.0564 & -22.77 \\ 17.9K_1 & 17.9K_2 & 17.9K_3 & 17.9K_4 & 17.9K_5 & 17.9K_6 & 17.9K_7 & (s+17.9+17.9K_8) \end{vmatrix} = 0$$

Expanding the above expression and comparing like coefficients of Equation 95 results in the following:

K_1 = -6.5929 $\quad K_2$ = -4.6841 $\quad K_3$ = 3.1998 $\quad K_4$ = .058693

K_5 = .01716 $\quad K_6$ = .00916 $\quad K_7$ = .002555 $\quad K_8$ = .1246

With these feedback gains, the feedback control law becomes

$$u = -Kx = 6.5929\phi + 4.6841\dot{\phi} - 3.1998\alpha - .058693\eta_1 - .01716\dot{\eta}_1 - .00916\eta_2 - .002555\dot{\eta}_2 - .1246\beta_L \tag{99}$$

Of the state variables in the control law (Equation 99), only β_L can be measured directly. Two methods for synthesizing the control law are presented in Reference 4.

REFERENCES

1. Data Received from the George C. Marshall Space Flight Center: Model Vehicle No. 2 for Advanced Control Studies.

2. Young, Dana: Generalized Missile Dynamics Analysis, II - Equations of Motion. Space Technology Laboratories CM-TR-0165-00359. 7 April 1958.

3. Lukens, D. R., A. F. Schmitt and G. T. Broucek: Approximate Transfer Functions for Flexible-Booster-and-Autopilot Analysis. WADD TR-61-93, April 1961.

4. Rynaski, E. G.: Study of Application of Optimal Control Theory and Design Techniques to the Control of a Highly Elastic Vehicle. (Monthly Progress Report), Contract NAS8-20067, September 1965.

5. Rynaski, E. G. and R. F. Whitbeck: The Theory and Application of Linear Optimal Control. CAL Report No. IH-1943-F-1 (AFFDL-TR-65-28), October 1965.

TABLE I

TRAJECTORY DATA AT t = 80 SECONDS (REFERENCE 1)

$F = 5,819,805$ kg

$X = 227,178$ kg

$m = 266051.2$ kg-sec^2/m

$\bar{q} = 3841$ kg/m^2

$V = 519.3$ m/sec

$M = 1.767$

$C_{z_{\alpha_{M=1.767}}} = 4.83$ 1/rad

$A = 79.5$ m^2

$x_{CP} = 53$ m

$x_{CG} = 41.5$ m

$I_y = 252 \times 10^6$ kg-m-sec^2

TABLE II

ENGINE DATA (REFERENCE 1)

$I_e = 3456.38$ kg-m-sec^2 (one engine, pitch or yaw)

$m_e = 925.07$ kg-sec^2/m (one engine)

$x_e = 1.33858$ m

$x_\beta = 2.54$ m

$R' = 1/2$ F

TABLE III

BENDING DATA AT t = 80 SECONDS (REFERENCE 1)

Bending Mode	Frequency (rad/sec)	Damping Ratio	Generalized Mass ($kg\text{-}sec^2/m$)
First	2.317	.005	170,748.1
Second	5.639	.005	115,674.3
Third	9.179	.005	98,114.7
Fourth	12.5	.005	565,743.8

TABLE IV

NORMALIZED DISPLACEMENTS AND SLOPES
AT t = 80 SECONDS (REFERENCE 1)

Location	Y_1	Y_1'	Y_2	Y_2'	Y_3	Y_3'	Y_4	Y_4'
0 m	1.0	.03563	1.0	.04727	1.0	.05660	1.0	.06362
2.54	.92869	.03569	.90509	.04764	.88583	.05758	.87095	.06544
4.54	.85725	.03573	.80950	.04788	.76990	.05818	.73864	.06654
6.54	.78569	.03590	.71321	.04878	.65226	.06038	.60333	.07037
8.54	.71359	.03619	.61403	.05033	.52773	.06397	.45623	.07634
10.54	.64096	.03642	.51220	.051428	.39729	.06625	.29982	.07961
12.54	.56795	.03657	.40870	.05197	.26381	.06695	.13990	.07977
14.54	.49493	.03643	.30541	.05118	.13163	.06498	-.01645	.07625
16.54	.42230	.03619	.20423	.04995	.00446	.06207	-.16423	.07133
18.54	.35020	.03590	.10583	.04839	-.11612	.05840	-.30095	.06519
20.54	.27818	.03626	.00796	.05016	-.23514	.06215	-.43455	.07078
22.54	.20636	.03554	-.08870	.04641	-.35094	.05346	-.56208	.05644
24.54	.13608	.03472	-.17730	.04208	-.44804	.04330	-.65878	.03952
26.54	.06905	.03317	-.24862	.03349	-.50418	.02215	-.68654	.00267
28.54	.00317	.03270	-.31244	.03026	-.53929	.01288	-.67400	-.01522
30.54	-.06168	.03214	-.36944	.02669	-.55543	.00324	-.62599	-.03265
32.54	-.12534	.03150	-.41899	.02283	-.55221	-.00643	-.54436	-.04869
34.54	-.18764	.03079	-.46063	.01878	-.52993	-.01577	-.43279	-.06248
36.54	-.24844	.03002	-.49416	.01495	-.48992	-.02353	-.29691	-.07223
38.54	-.30776	.02929	-.52120	.01210	-.43829	-.02800	-.14774	-.07670
40.54	-.36556	.02851	-.54258	.00929	-.37832	-.37832	-.00882	-.07962
42.54	-.42176	.02768	-.55838	.00652	-.31121	-.03513	.16969	-.08101
44.54	-.47627	.02682	-.56867	.00379	-.23820	-.03779	.33177	-.08084
46.54	-.52900	.02591	-.57356	.00111	-.16048	-.03983	.49199	-.07914

TABLE IV (CONTINUED)

Location	Y_1	Y'_1	Y_2	Y'_2	Y_3	Y'_3	Y_4	Y'_4
48.54	-.58057	.02518	-.57065	-.00443	-.06234	-.05526	.68639	-.10592
50.54	-.62880	.02303	-.55620	-.01001	.05015	-.05702	.88844	-.09562
52.54	-.67258	.02055	-.53078	-.01504	.16377	-.05317	1.06395	-.07167
54.54	-.71176	.01863	-.49622	-.01950	.26953	-.05242	1.19367	-.05759
56.54	-.74704	.01662	-.45282	-.02389	.37264	-.05051	1.29210	-.04040
58.54	-.77778	.01403	-.39924	-.02985	.46701	-.04300	1.33109	.00517
60.54	-.80310	.01128	-.33364	-.03566	.54309	-.03284	1.26940	.05629
62.54	-.82290	.00852	-.25705	-.04082	.59754	-.02146	1.10849	.10381
64.54	-.83757	.00623	-.17121	-.04471	.63371	-.01549	.87274	.12800
66.54	-.84787	.00409	-.07861	-.04783	.65986	-.01067	.59997	.14430
68.54	-.85393	.00198	.01983	-.05054	.67642	-.00590	.29760	.15759
70.54	-.85583	-.00008	.12327	-.05283	.68350	-.00120	-.02828	.16779
72.54	-.85363	-.00210	.23087	-.05471	.68132	.00336	-.37143	.17487
74.54	-.84744	-.00408	.34181	-.05617	.67018	.00775	-.72561	.17882
76.54	-.83736	-.00600	.45525	-.05721	.65045	.01194	-1.08458	.17968
78.54	-.82348	-.00787	.57039	-.05786	.62257	.01590	-1.44224	.17752
80.54	-.80264	-.01319	.70000	-.06906	.57488	.03104	-1.87573	.23626
82.54	-.77166	-.01776	.83839	-.06921	.50475	.03892	-2.33486	.22220
84.54	-.73244	-.02155	.97139	-.06402	.42347	.04265	-2.73004	.17419
86.54	-.68494	-.02606	1.09510	-.05962	.33302	.04791	-3.03430	.12935
88.54	-.62770	-.03133	1.20939	-.05441	.23130	.05398	-3.24263	.07633
90.54	-.55890	-.03751	1.31055	-.04666	.11574	.06161	-3.31212	-.00799
92.54	-.47783	-.04351	1.39530	-.03796	-.01385	.06767	-3.20899	-.09493
94.54	-.38513	-.04911	1.46270	-.02997	-.15363	.07192	-2.94327	-.16361

TABLE IV (CONCLUDED)

Location	Y_1	Y'_1	Y_2	Y'_2	Y_3	Y'_3	Y_4	Y'_4
96.54	-.28164	-.05433	1.51575	-.02306	-.30064	.07486	-2.56652	-.21212
98.54	-.16803	-.05923	1.55482	-.01599	-.45211	.07638	-2.09945	-.25385
100.54	-.04495	-.06380	1.57966	-.00884	-.60522	.07651	-1.55606	-.28839
102.54	.08697	-.06806	1.59013	-.00163	-.75723	.07529	-.95108	-.31539
104.54	.22707	-.07199	1.58619	.00557	-.90550	.07278	-.29982	-.33464
106.54	.37471	-.07560	1.56788	.01272	-1.04751	.06905	.38205	-.34600
108.54	.53020	-.08271	1.53464	.02269	-1.18311	.07299	1.09672	-.42140
110.54	.73093	-.09089	1.47034	.04143	-1.31345	.05716	1.93131	-.41047
112.54	.89320	-.09823	1.36944	.05939	-1.41034	.03933	2.72556	-.38067
114.54	1.09628	-.10472	1.23315	.07681	-1.46905	.01901	3.44045	-.33117
116.54	1.31126	-.10988	1.06147	.09601	-1.48083	-.01204	4.01787	-.22122
118.54	1.53502	-.11403	.84921	.11487	-1.41705	-.04725	4.29693	-.07974
120.54	1.76733	-.11818	.60480	.12927	-1.29939	-.07015	4.37131	.00520
122.54	2.00746	-.12191	.33288	.14253	-1.13723	-.09189	4.27669	.08937
124.54	2.25505	-.12577	.03420	.15654	-.93050	-.11559	4.00599	.18490
126.54	2.51150	-.13091	-.29672	.17549	-.66896	-.14838	3.51170	.32192
128.54	2.77820	-.13557	-.66796	.19499	-.33290	-.18655	2.68403	.50219
130.54	3.05285	-.13888	-1.07344	.20977	.07211	-.21725	1.52149	.65557
132.54	3.33294	-.14106	-1.50403	.22016	.53069	-.24010	.08470	.77567
134.54	3.61652	-.14251	-1.95169	.22728	1.02756	-.25607	-1.55685	.86125
136.54	3.90255	-.14342	-2.41118	.23177	1.55078	-.26621	-3.33877	.81591
138.54	4.18980	-.14376	-2.87695	.23363	2.08852	-.27072	-5.20052	.94156
140.54	4.47723	-.14358	-3.34409	.23305	2.63014	-.26988	-7.08634	.93886
142.54	4.76411	-.14333	-3.80895	.23199	3.16740	-.26773	-8.95187	.92335
144.54	5.05052	-.14306	-4.27173	.23065	3.70022	-.26476	-10.79460	.91249

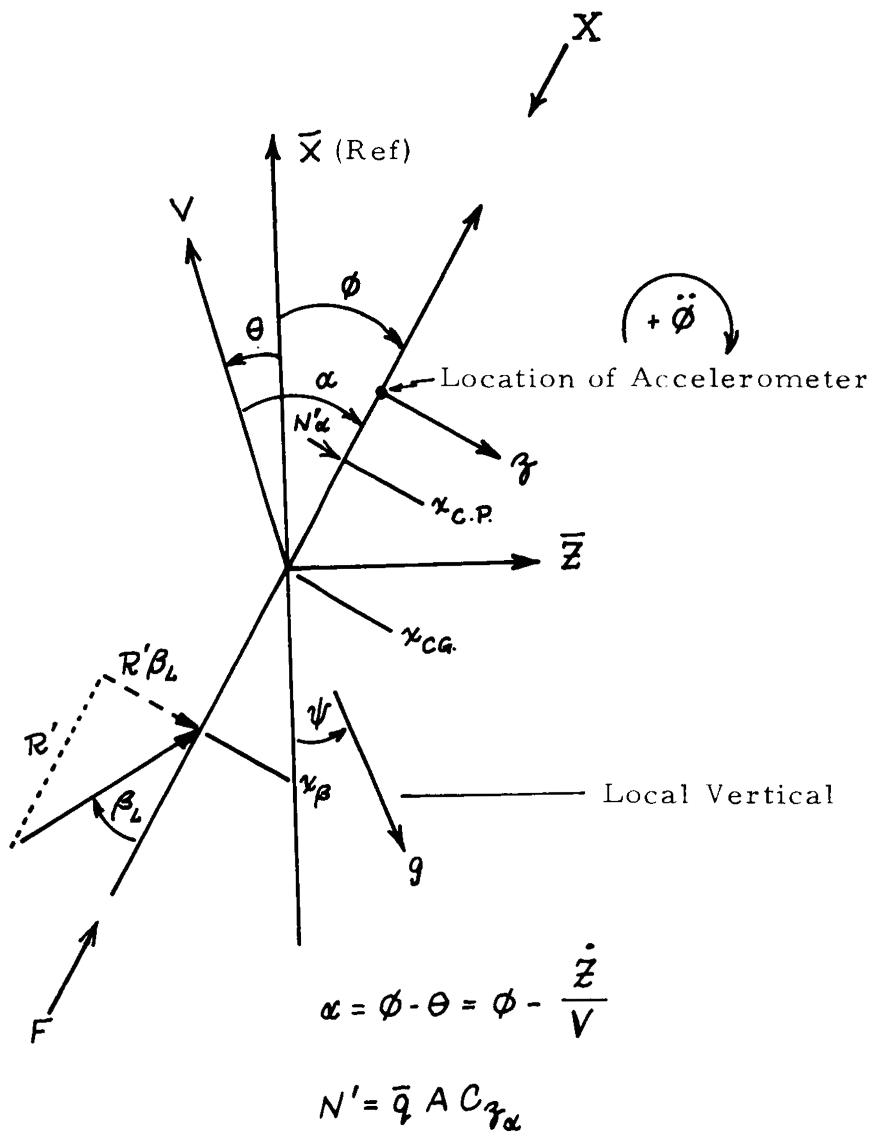

Figure 1 Rigid-Body Coordinate System

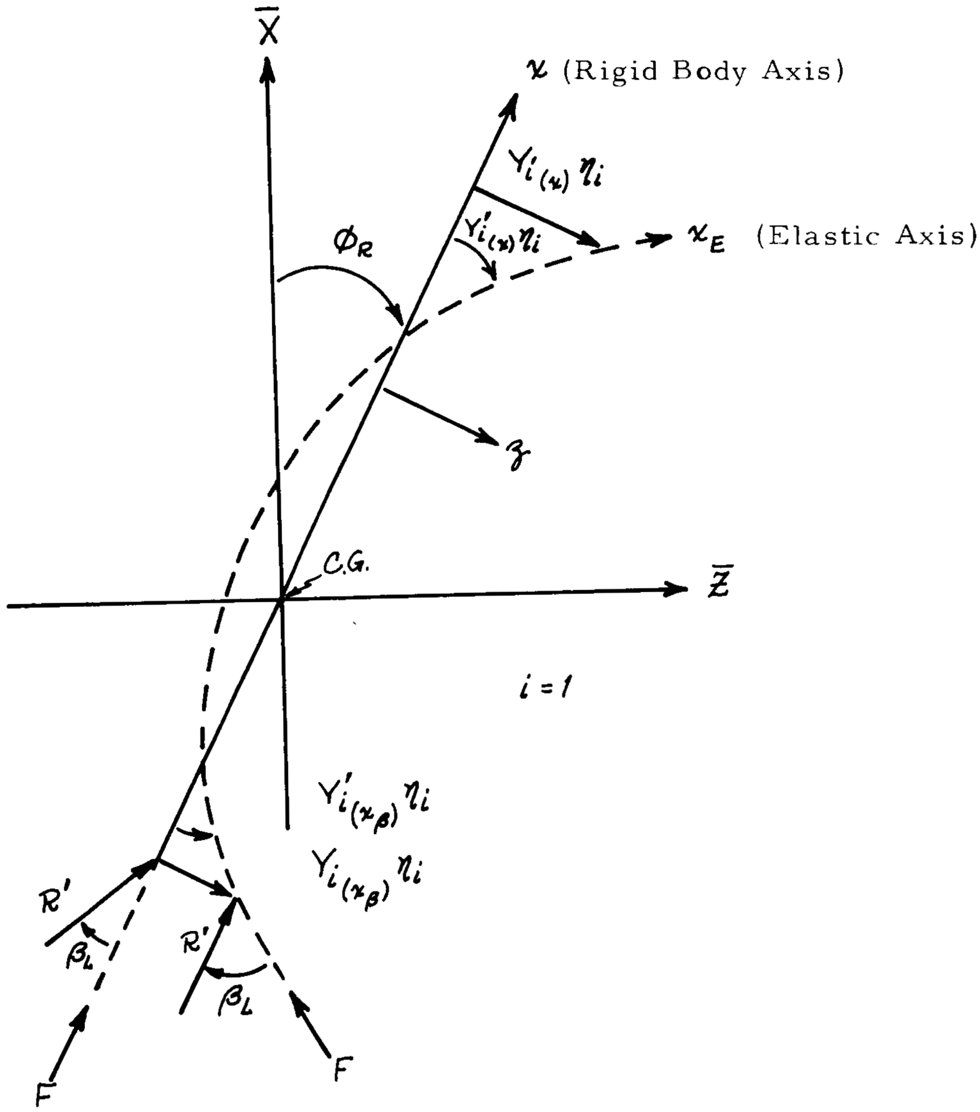

Figure 2 First Bending Mode Geometry

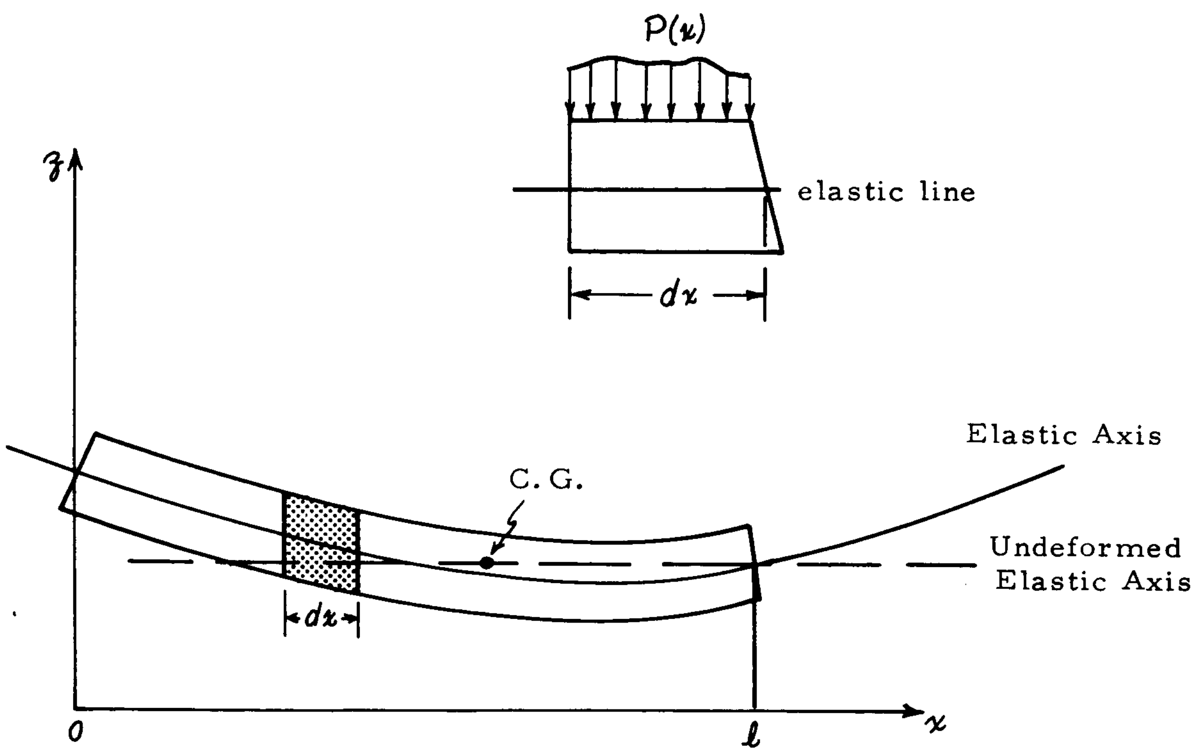

Figure 3 Elastic Beam Coordinates

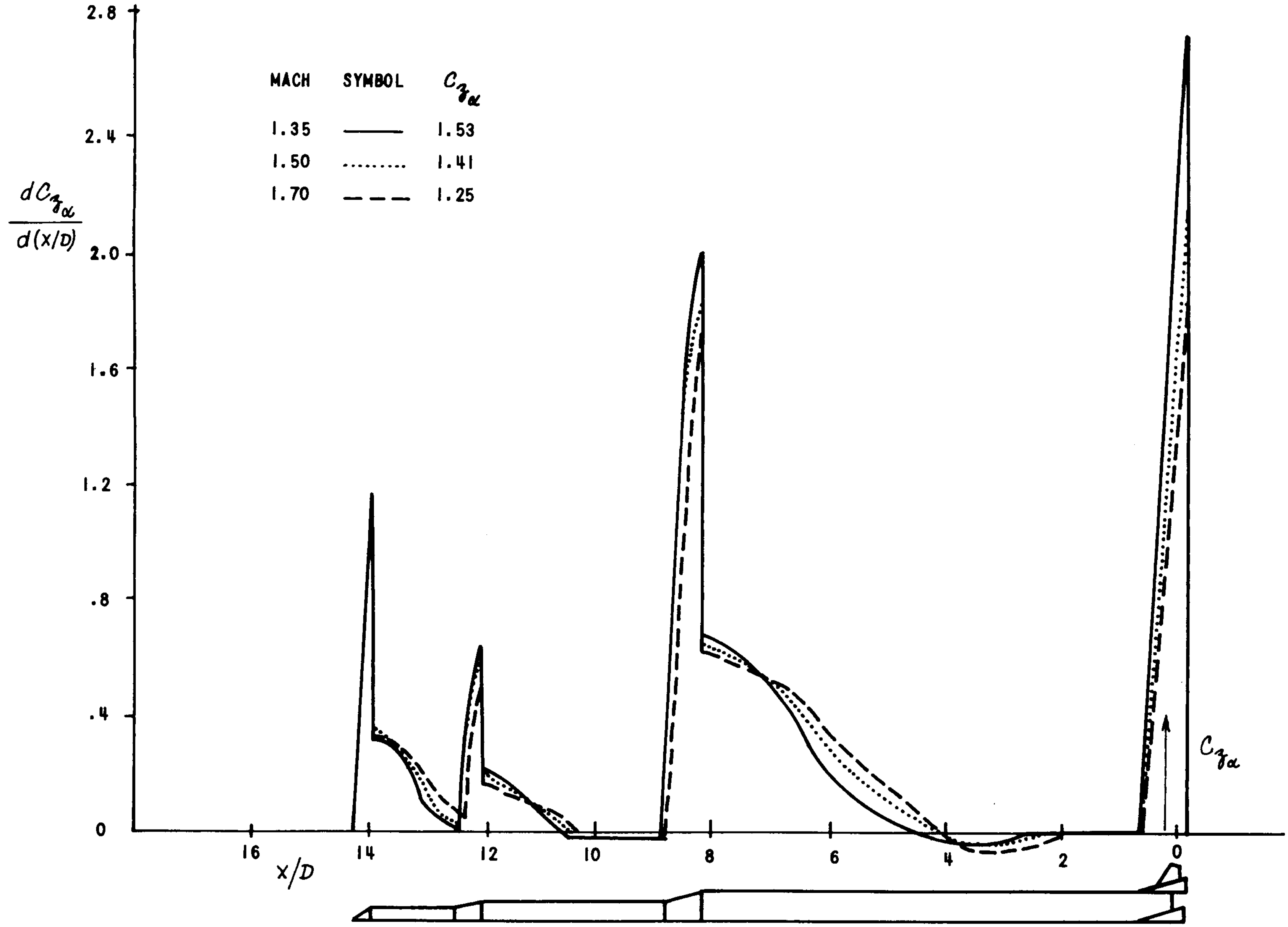

Figure 4 Distribution of Local Normal Force for Model Vehicle No. 2

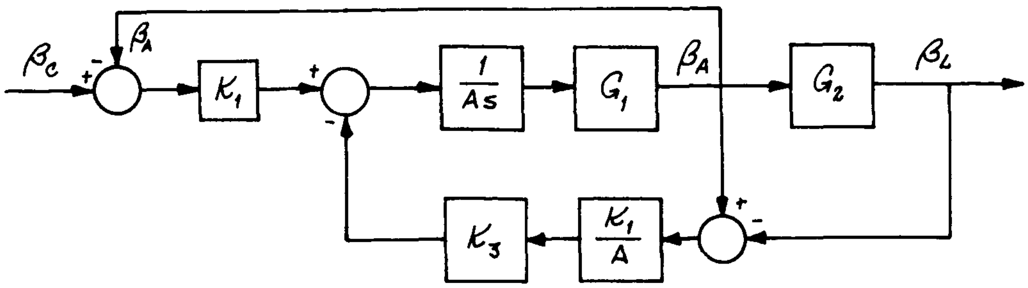

Figure 5 Block Diagram of Engine-Actuator System

$$G_1 = \frac{\dfrac{K_0}{K_0 + K_L}\left(s^2 + \dfrac{B_L}{M_L}\, s + \dfrac{K_L}{M_L}\right)}{s^2 + \dfrac{B_L}{M_L}\, s + \dfrac{K_L K_0}{(K_L + K_0) M_L}}$$

$$G_2 = \frac{\beta_L}{\beta_A} = \frac{\dfrac{K_L}{M_L}}{s^2 + \dfrac{\beta_L}{M_L}\, s + \dfrac{K_L}{M_L}}$$

K_3 = valve pressure feedback gain

K_1 = open-loop gain

K_0 = effective hydraulic spring constant

K_L = effective load spring constant

M_L = effective load mass

B_L = real damping at gimbal

β_c = actuator command

β_A = actuator output

β_L = control engine gimbal angle

(Taken from Reference 1)

$$\frac{\beta_L}{\beta_c} = \frac{\dfrac{K_1 K_o K_L}{A(K_o+K_L)M_L}}{s^3 + s^2\left[\dfrac{B_L}{M_L} + \dfrac{K_3 K_L K_o}{(K_o+K_L)A^2} + \dfrac{K_1 K_o}{A(K_o+K_L)}\right] + s\left[\dfrac{K_L K_o}{(K_o+K_L)M_L} + \dfrac{K_3 K_L K_o B_L}{(K_o+K_L)A^2 M_L} + \dfrac{K_1 K_o B_L}{A(K_o+K_L)M_L}\right] + \dfrac{K_1 K_o K_L}{A(K_o+K_L)M_L}}$$

$$\frac{\beta_L}{\beta_c} = \frac{38.912\,K_1}{s^3 + s^2(11.816 + .01488\,K_1) + s(2236.5 + .028034\,K_1) + 38.912\,K_1}$$

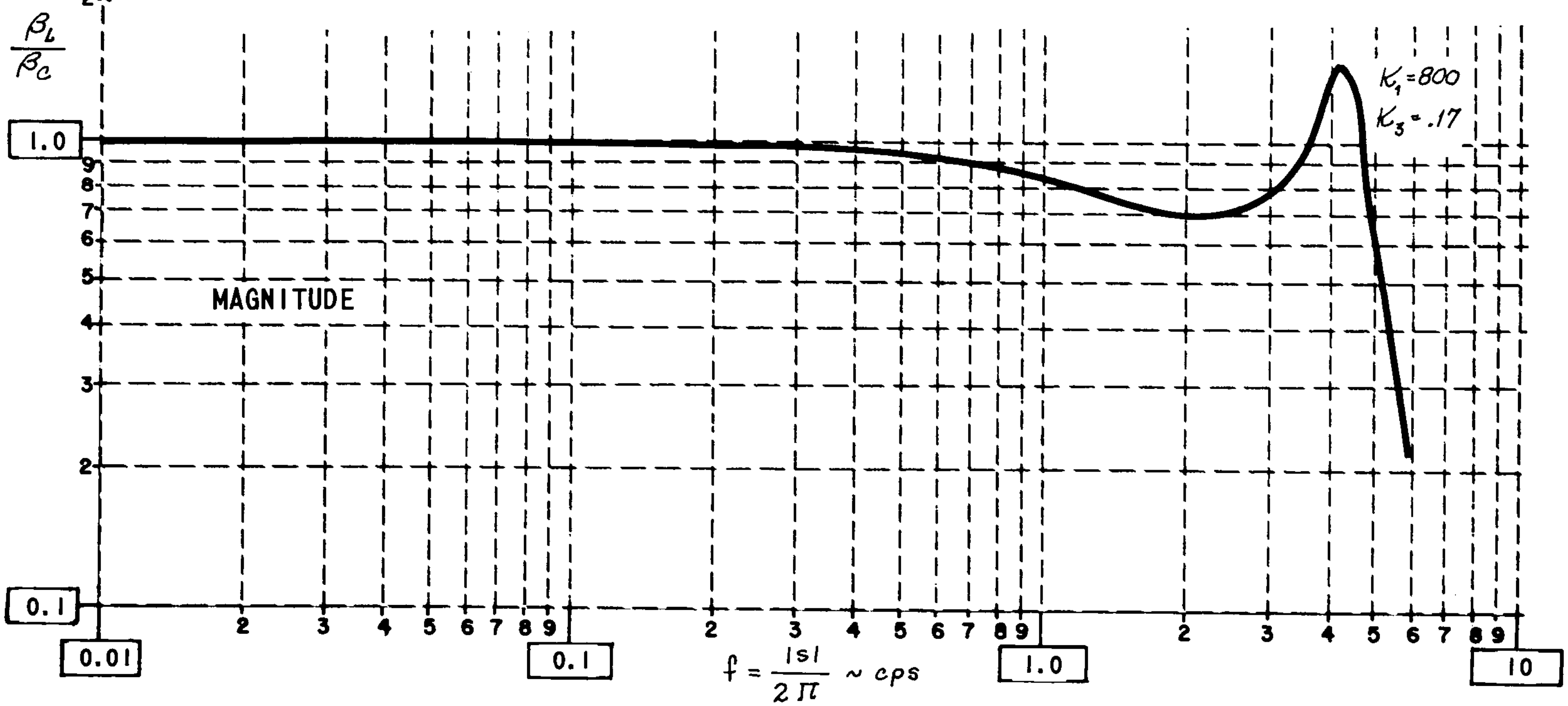

Figure 6 Engine-Actuator Frequency Response Plot - Magnitude

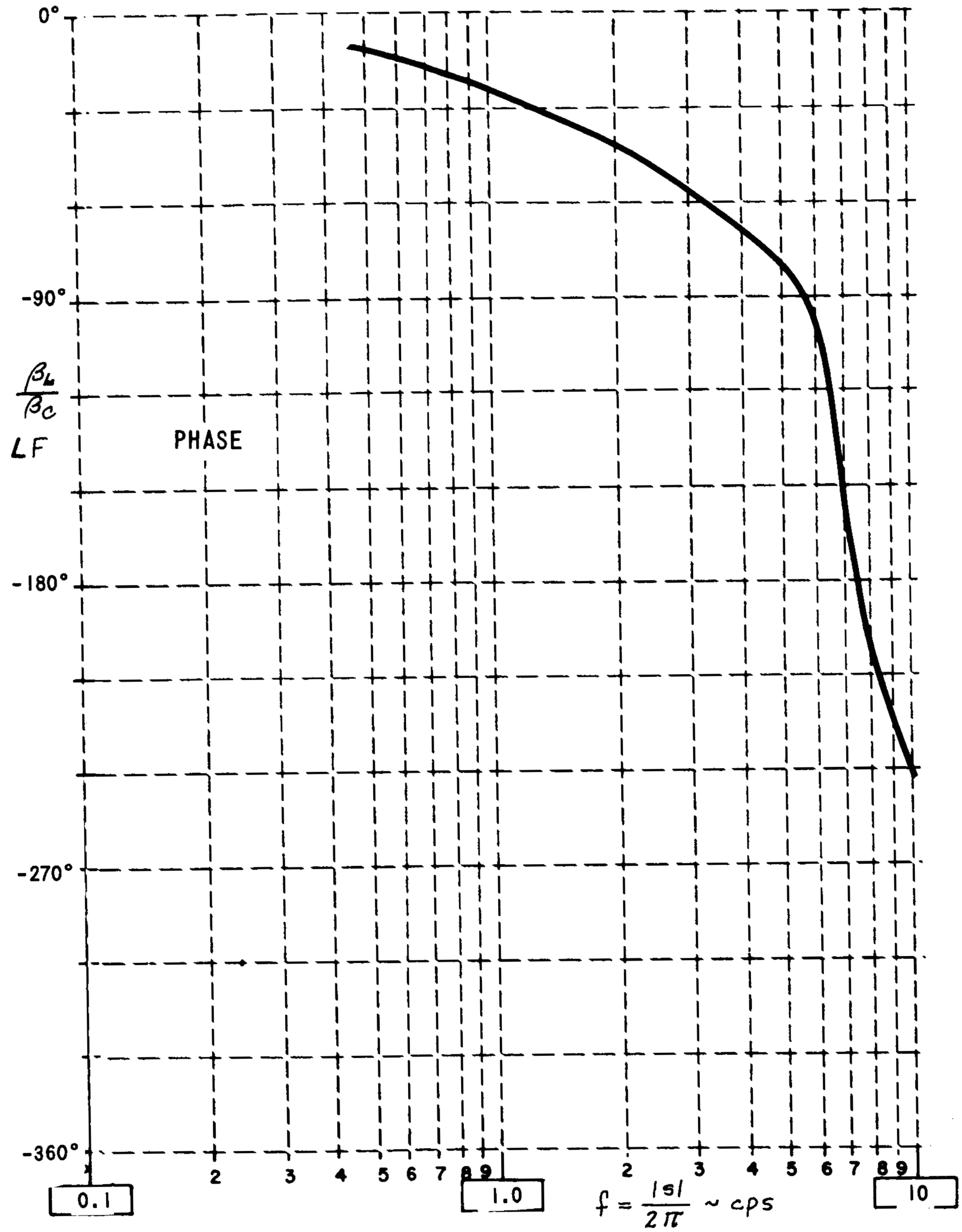

Figure 7 Engine-Actuator Frequency Response Plot - Phase

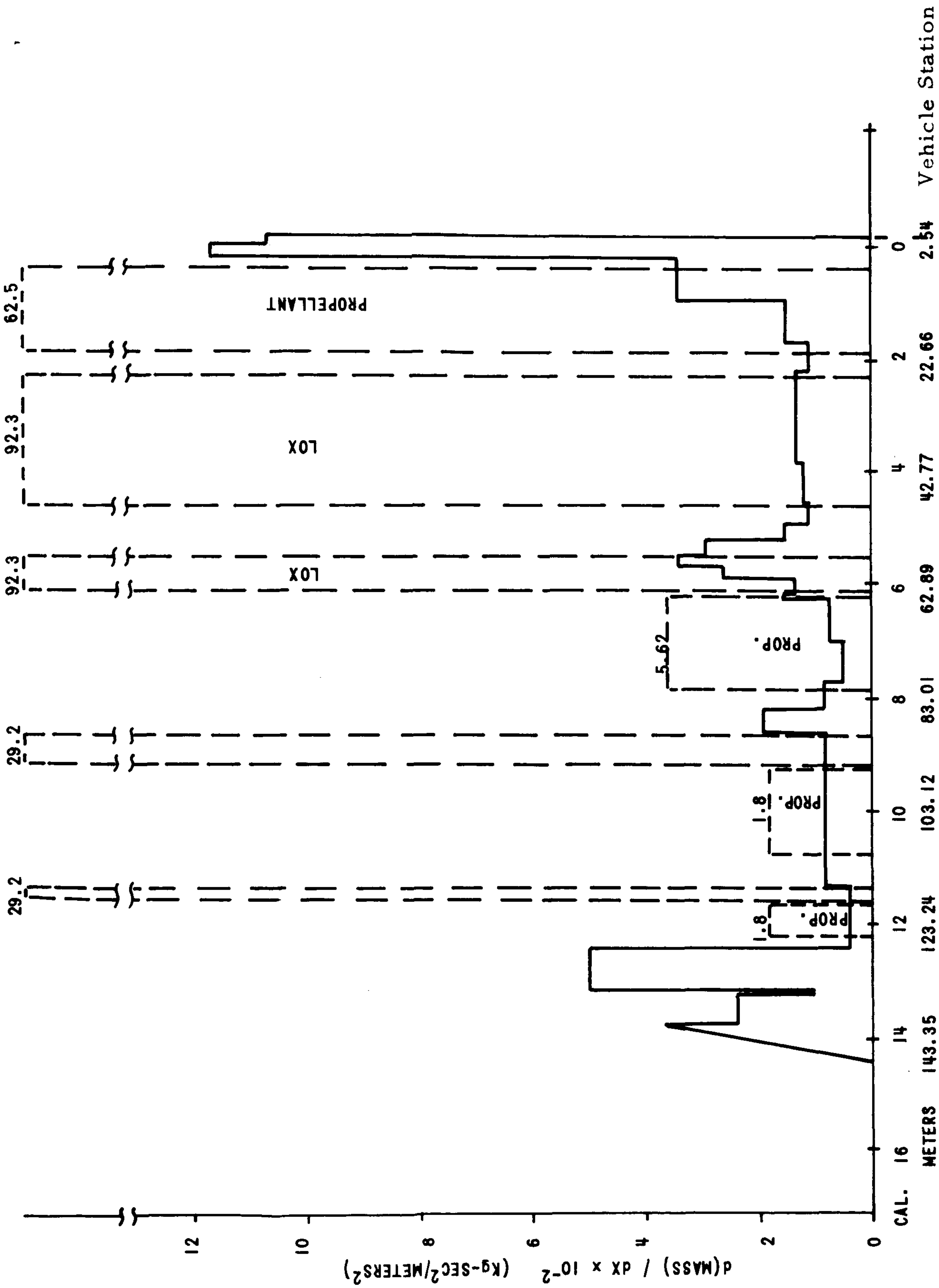

Figure 8 Model Vehicle Mass Distribution

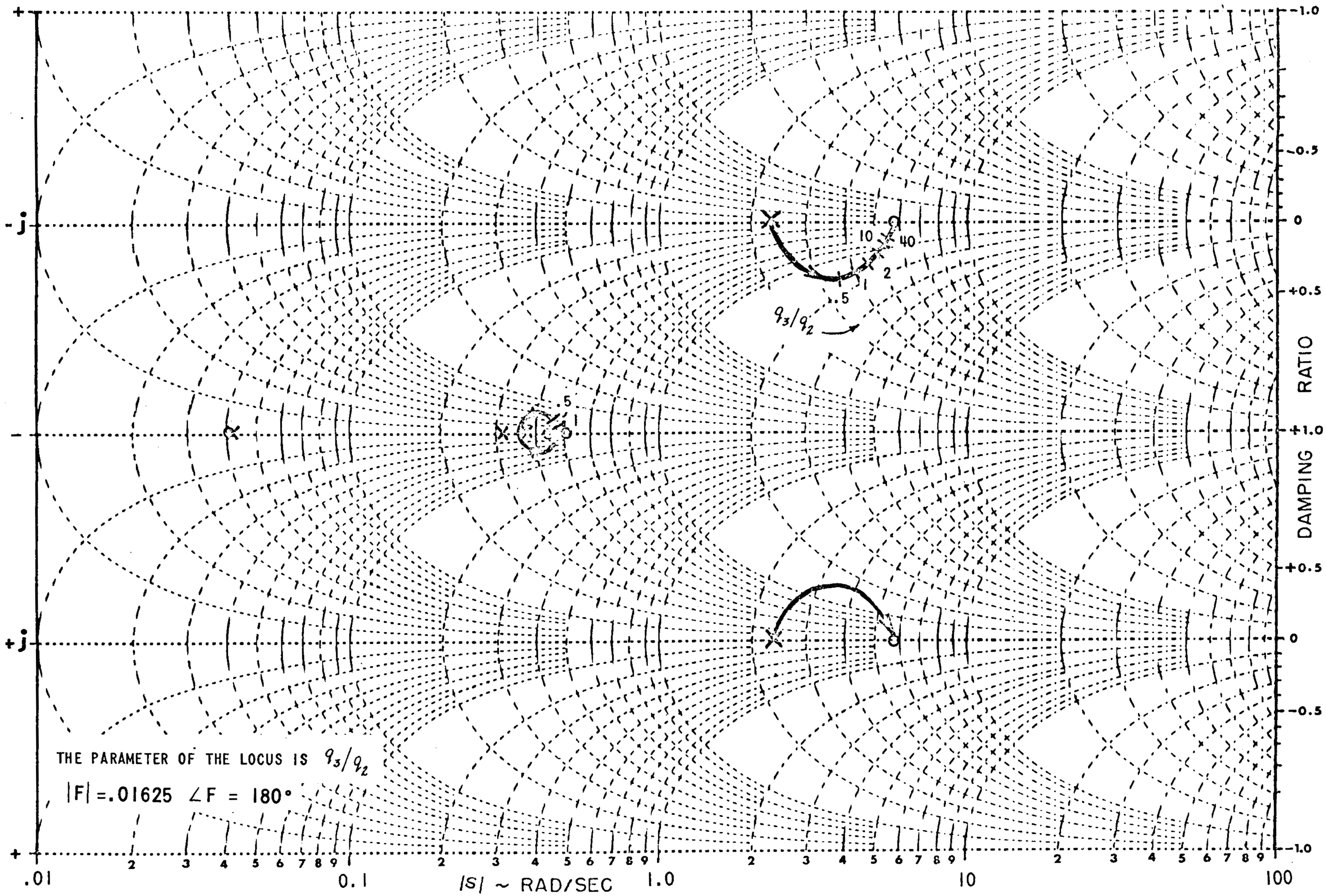

Figure 9 Root Square Locus Plot of Equation 91

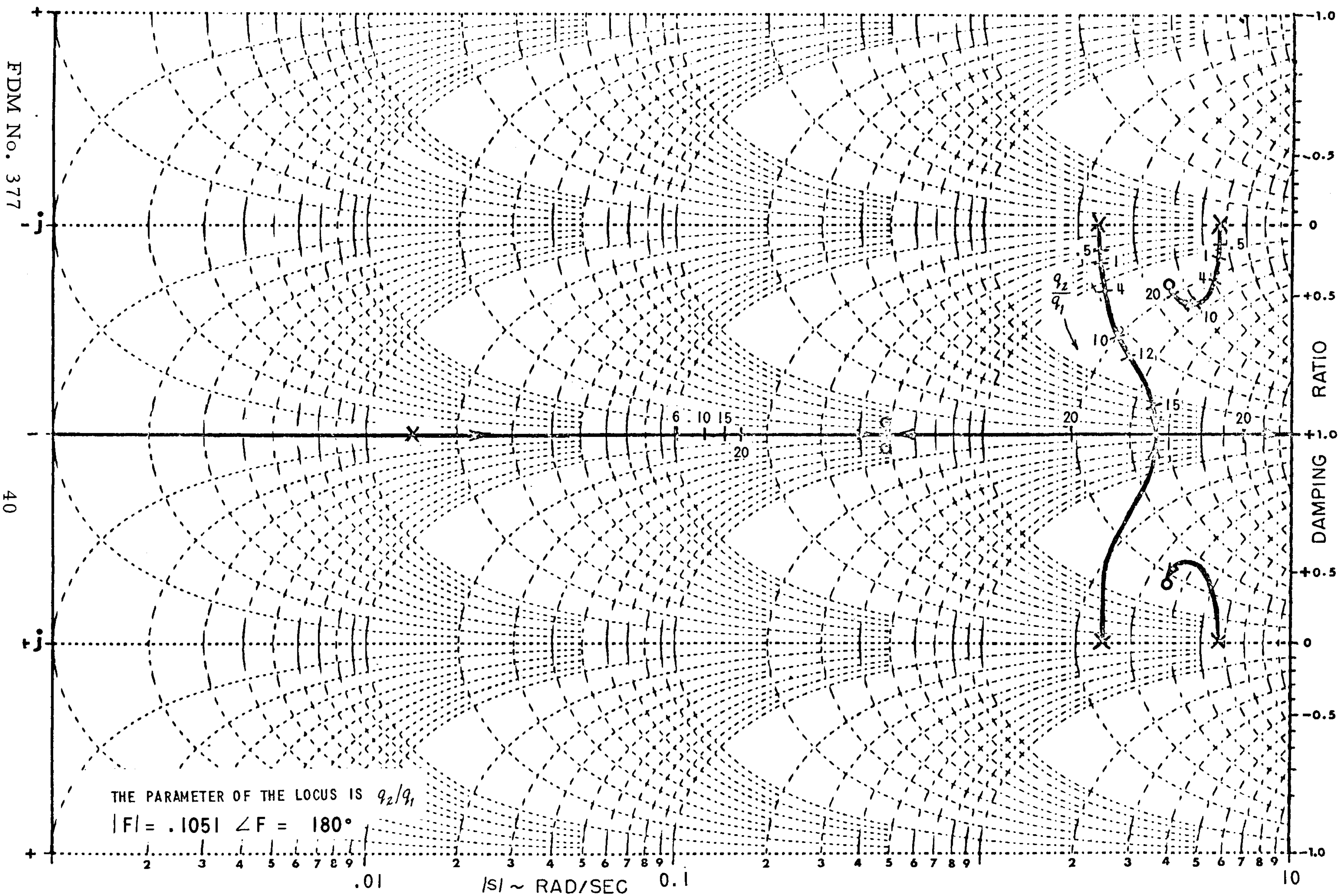

Figure 10 Root Square Locus Plot of Equation 92

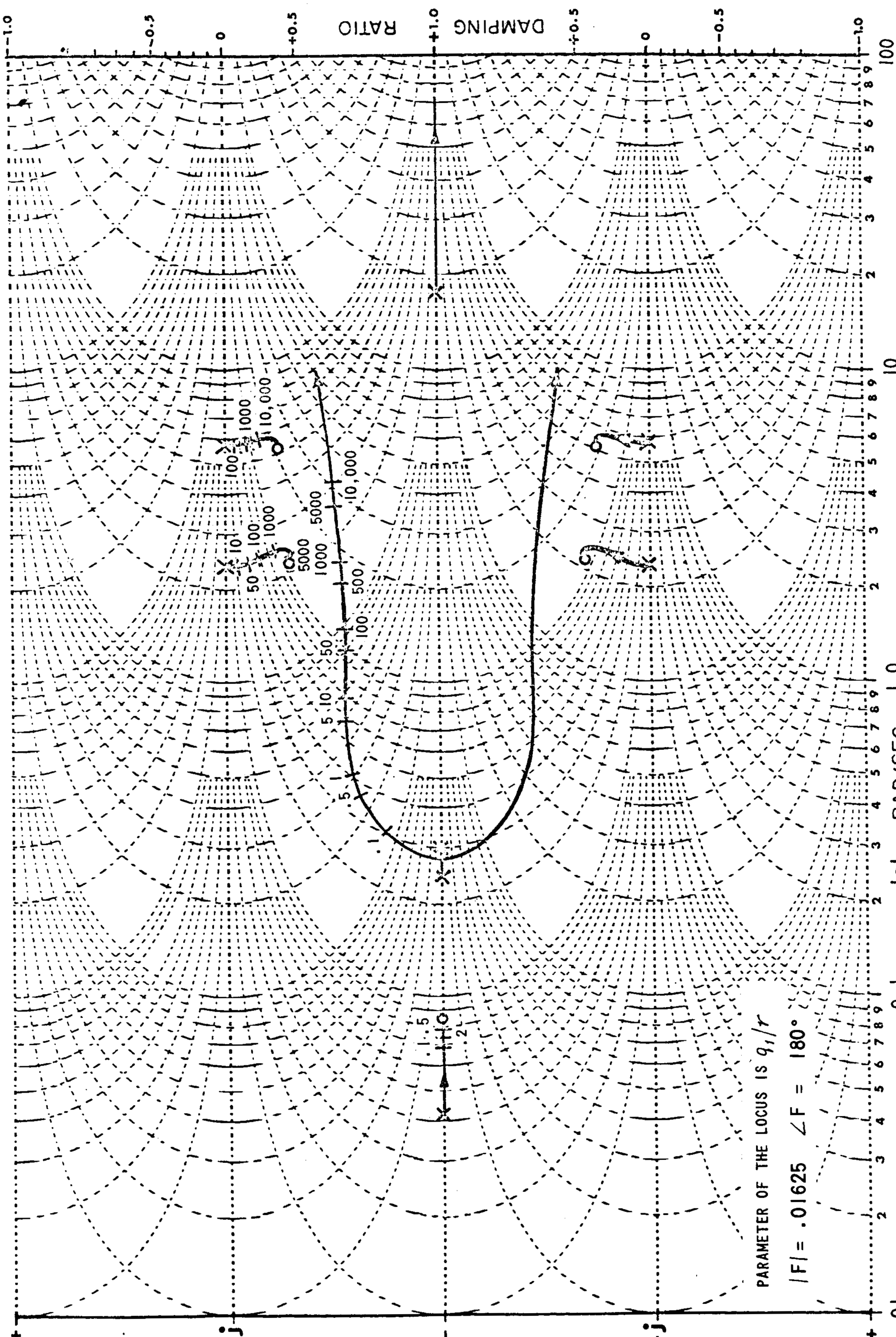

Figure 11 Locus of the Poles of the Closed-Loop Optimal System